Electronic Supplementary Material (ESI) for Inorganic Chemistry Frontiers.

Enhancing photoluminescence efficiency of atomically precise copper(I) nanoclusters through solvent-induced structural transformation

Su-Kao Peng, [+] Hu Yang, [+] Dong Luo, Mo Xie, Wen-Jing Tang, Guo-Hong Ning* and Dan Li*

[+]S.-K. P. and H. Y. contributed equally to this work

College of Chemistry and Materials Science, Guangdong Provincial Key Laboratory of Functional Supramolecular Coordination Materials and Applications, Jinan University, Guangzhou 510632, China.
E-mail: guohongning@jnu.edu.cn, danli@jnu.edu.cn

Experiment detail

Material and method.

All starting materials and solvents were purchased from commercial sources and without further purification. Element analysis was carried out by Elementar Vario Micro Cube. Fourier-transfer infrared (FT-IR) spectra were recorded on a Thermo Scientific FT-IR Nicolet iS_{10} spectrophotometer from 4000 cm^{-1} to 400 cm^{-1}. The solid-state ultraviolet-visible (UV-vis) absorption spectra were recorded on the Bio-Logic MOS-500 multifunctional circular dichroism spectrometer, while solution UV-vis absorption spectra were measured by Agilent Cary 4000 UV-Vis spectrophotometer. Rigaku Ultima IV X-ray diffractometer, using the Cu Kα (λ = 1.5418 Å, step = 0.02°), collected the data of powder x-ray diffraction under the conditions 40 kV and 40 mA. Thermogravimetric analysis (TGA) was performed on TGA Q50 V20.6 with N_2 atmosphere heating rate of 10 ℃/min and temperatures ranging from 40 ° C to 800 ° C. The NMR signals were recorded by Bruker Ascend 400, using CD_2Cl_2 as solvent. X-ray photoelectron spectroscopy (XPS) was performed by Thermo Scientific™ K-Alpha™. ESI-MS spectra were recorded with a Waters Synapt G2-Si mass spectrometer and all the samples were dissolved in HPLC-grade dichloromethane before performing mass spectrometric analyses.

Horiba FluoroMax-4 fluorometer was used for steady-state photoluminescence spectra measurement for all samples and Janis VPF-100 cryostat system was used for temperature-controlled measurement by adopting liquid nitrogen. The Decay curves were recorded by an Edinburgh FLS920 spectrometer, which is equipped with a μF900 μs flash lamp and a closed-cycle cryostat (Advanced Research Systems) using liquid helium as a cooling medium. Hamamatsu C11347-01 absolute PL quantum yield spectrometer was used for the absolute photoluminescence quantum yields measurement under room temperature. The crystal samples were used for all photoluminescence measurements in solid sample states, and the crystal phase purity of the samples was ensured by elemental analysis and powder X-ray diffraction measurements.

Single-crystal data were collected on an Oxford Diffraction XtalAB [Rigaku (Cu) X-ray dual-wavelength source Kα, λ = 1.5418 Å] equipped with a monochromometer and CCD plate detector with a temperature of 100 K (CrysAlisPro CCD, Oxford Diffraction Ltd.). The structure was solved by the ShelXT[1] direct method in OLEX2 program package[2] and all non-hydrogen atoms were refined with anisotropically by the full-matrix least-square method on F2 by using the ShelXL program[3]. The treatment of disordered guest molecules in cavities involves the SQUEEZE program using PLATON. Crystal data and structure refinement parameters are summarized in Table S1. Selected bond lengths and angles are given in TableS2 – S4. CCDC nos. 2182733-2182738. The data are available free of charge from the Cambridge Crystallographic Data Centre.

Crystal structure and data

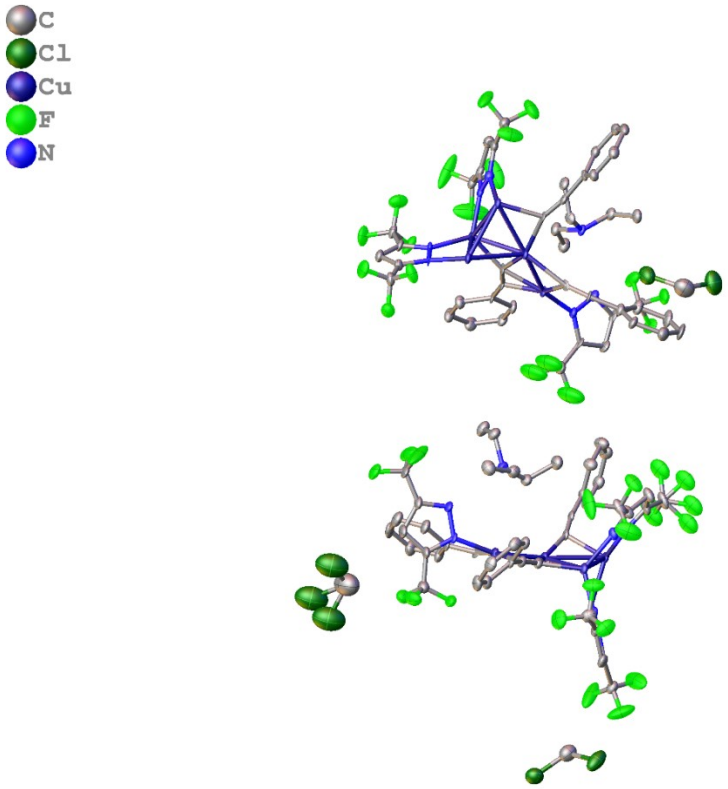

Fig. S1 The asymmetry unit of Cu_{10}.

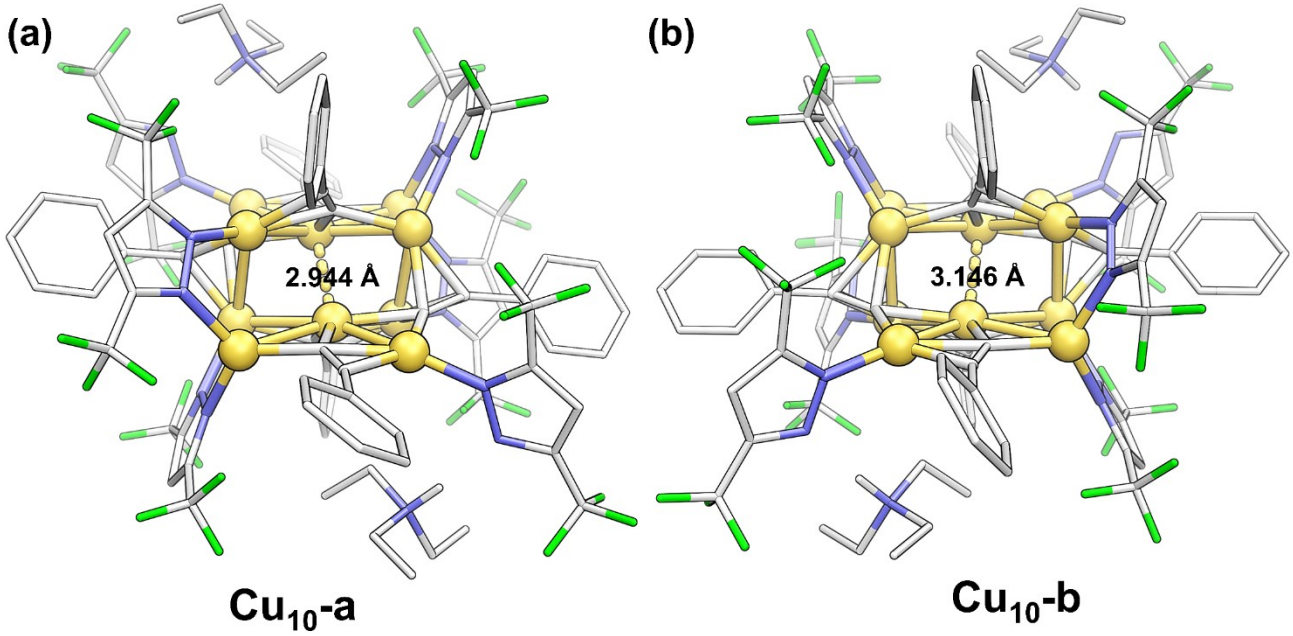

Fig. S2 The crystal structures of **Cu_{10}-a** and **Cu_{10}-b**, showing different Cu···Cu distance in **Cu_{10}** core.

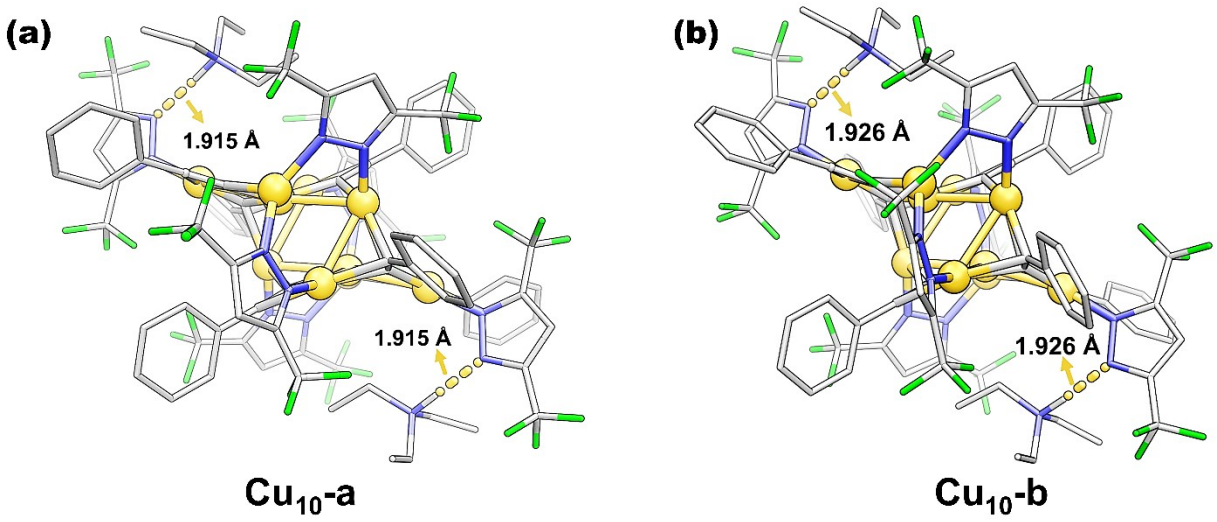

Fig. S3 The hydrogen bond formed between (a) **Cu_{10}-a**/(b) **Cu_{10}-b** and Et_3NH^+ cations.

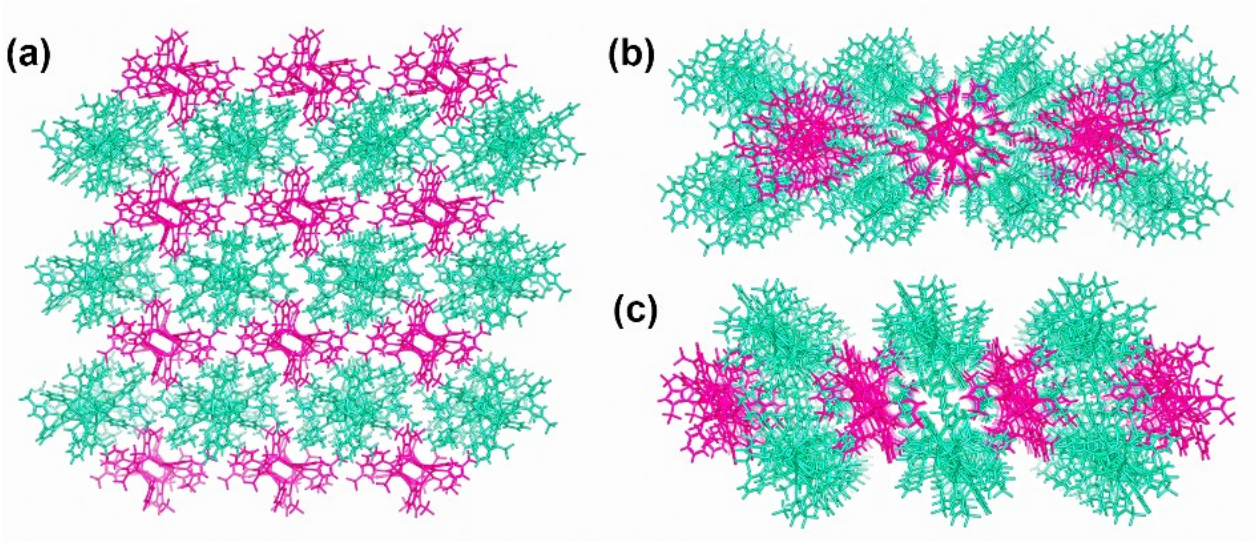

Fig. S4 The packing mode of **Cu_{10}** viewed from (a) a axis, (b) b axis and (c) c axis. Purple and cyan represent for **Cu_{10}-a** and **Cu_{10}-b**, respectively.

Table S1. Crystallographic data for **Cu_{10}** and **Cu_{18}**

	Cu_{10}	**Cu_{18}**
Empirical formula	$C_{93}H_{74}Cl_6Cu_{10}F_{36}N_{14}$	$C_{127}H_{68}ClCu_{18}F_{36}N_{12}$
Formula weight	2919.76	3612.40
Temperature (K)	100.00(16)	293 (2)
Wavelength (*Å*)	1.54184	1.54184
Crystal system	Triclinic	Monoclinic
space group	*P-1*	*P2(1)/n*
a (*Å*)	15.3985(3)	18.3419(2)

b (*Å*)	18.9186(3)	17.1774(2)
c (*Å*)	18.9345(4)	20.5081(3)
Volume ($Å^3$)	5395.91(18)	6460.80(14)
Z	2	2
ρ_{calc} （Mg/cm^3）	1.797	1.863
R_{int}	0.0749	0.035
Completeness (%)	99.5	99.7
Data / restraints / parameters	22099 / 9 / 1390	13212 / 174 / 787
Goodness-of-fit on F^2	1.016	1.064
R_1[a] [I>2sigma(I)]	0.0953	0.0970
wR_2[b] (all data)	0.2394	0.2587
Largest diff. peak and hole ($e/Å^3$)	4.447 , -2.192	2.637, -2.043

[a]$R_1 = \Sigma||F_o| - |F_c||/\Sigma|F_o|$.[b] $wR_2 = \{[\Sigma w(F_o^2-F_c^2)^2]/\Sigma[w(F_o^2)^2]\}^{1/2}$; $w = 1/[\sigma^2(F_o^2) + (aP)^2 + bP]$, where $P = [\max(F_o^2,0) + 2F_c^2]/3$ for all data.

Table S2. Comparisons of bond lengths (Å) in **Cu_{10}**, and **Cu_{18}**

Bond type	**Cu_{10}-a**	**Cu_{10}-b**
Cu-Cu	2.491~2.741	2.503~2.671
σ-type Cu-C	1.955 ~ 2.197	1.925~2.210
π-type Cu-C	2.028~2.243	2.024~2.299
Cu-N	1.939~1.994	1.931~1.995

Table S3. Comparisons of bond lengths (Å) in **Cu_{10}**, and **Cu_{18}**

Bond type	**Cu_{10}**	**Cu_{18}**
Cu-Cu	2.4910(13)- 2.7406(14)	2.4905(13) - 2.7335(13)
Cu-C	1.955(6) - 2.4910(13)	1.852(7) - 2.509(7)
Cu-N	1.934(6) - 1.996(6)	1.891(6) - 2.017(6)

NMR

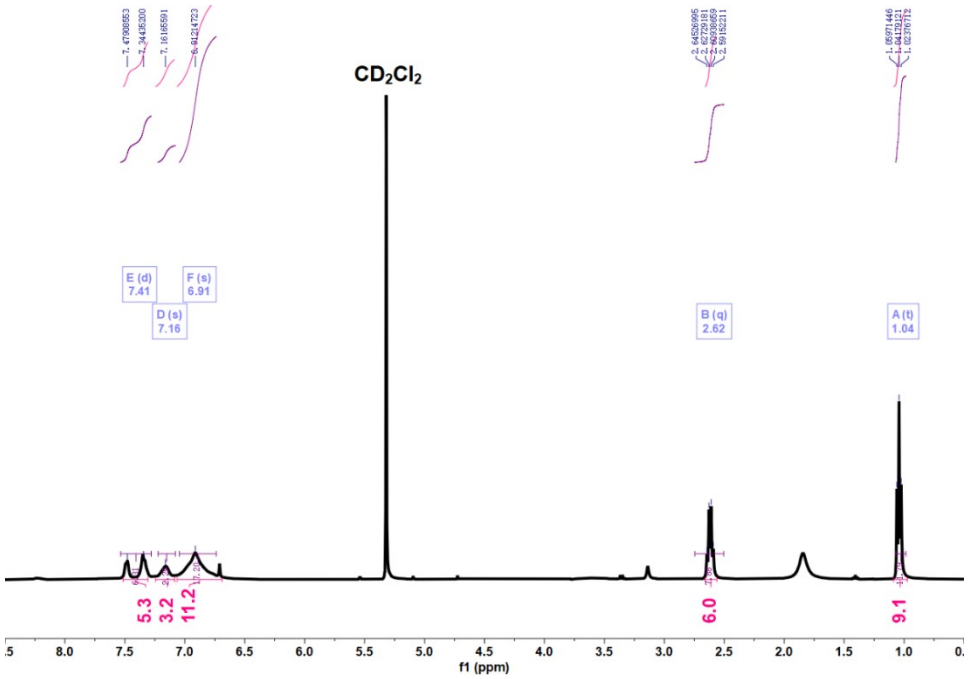

Fig. S5 ^{1}H NMR spectrum of **Cu$_{10}$** in CD_2Cl_2.

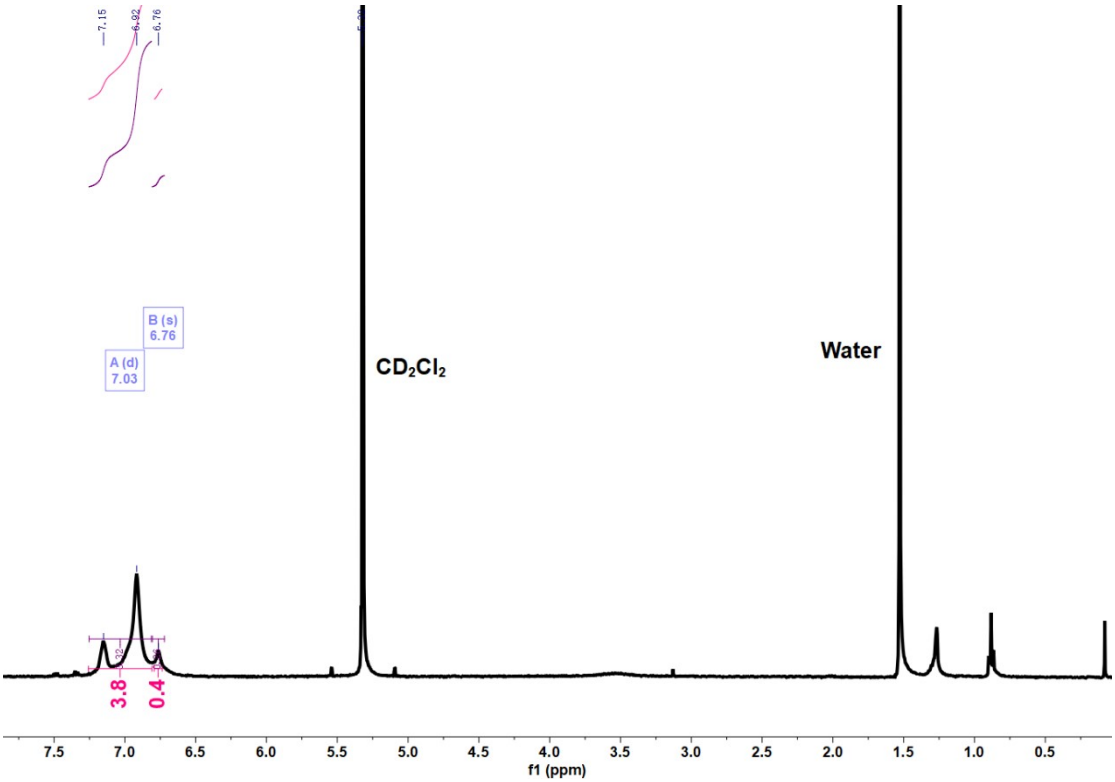

Fig. S6 ^{1}H NMR spectrum of **Cu$_{18}$** in CD_2Cl_2.

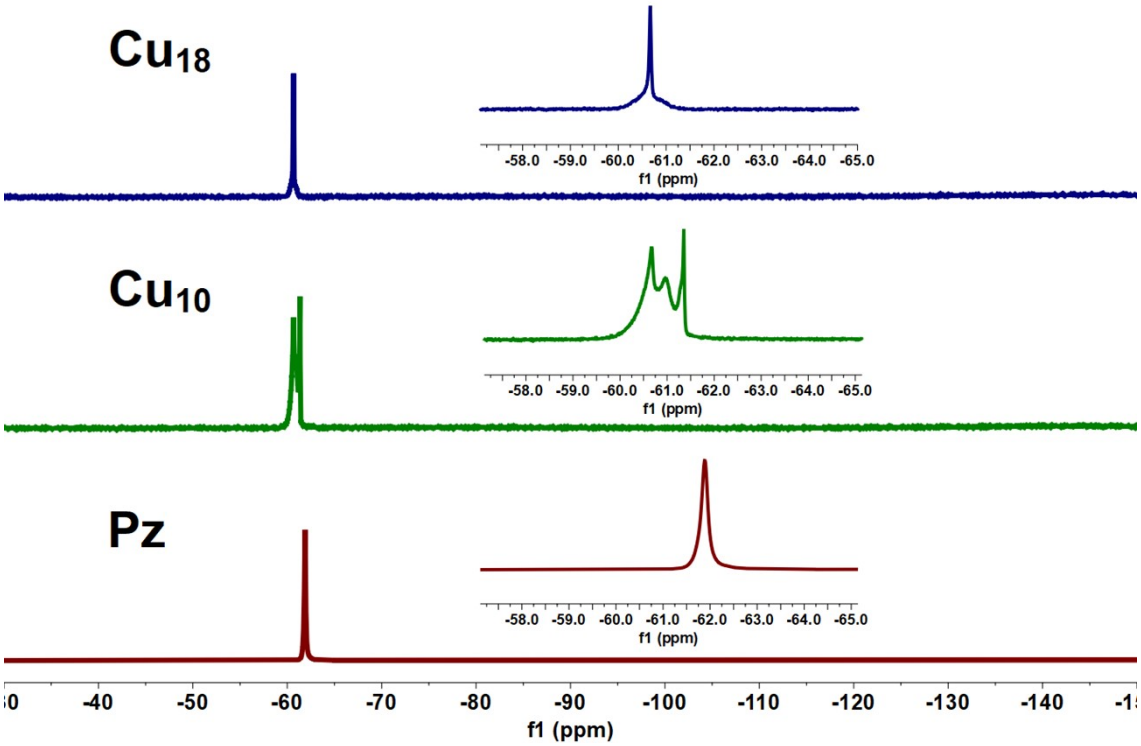

Fig. S7 ^{19}F NMR spectrum of 3,5-$(CF_3)_2$-pz, **Cu_{10}** and **Cu_{18}** in CD_2Cl_2.

MS

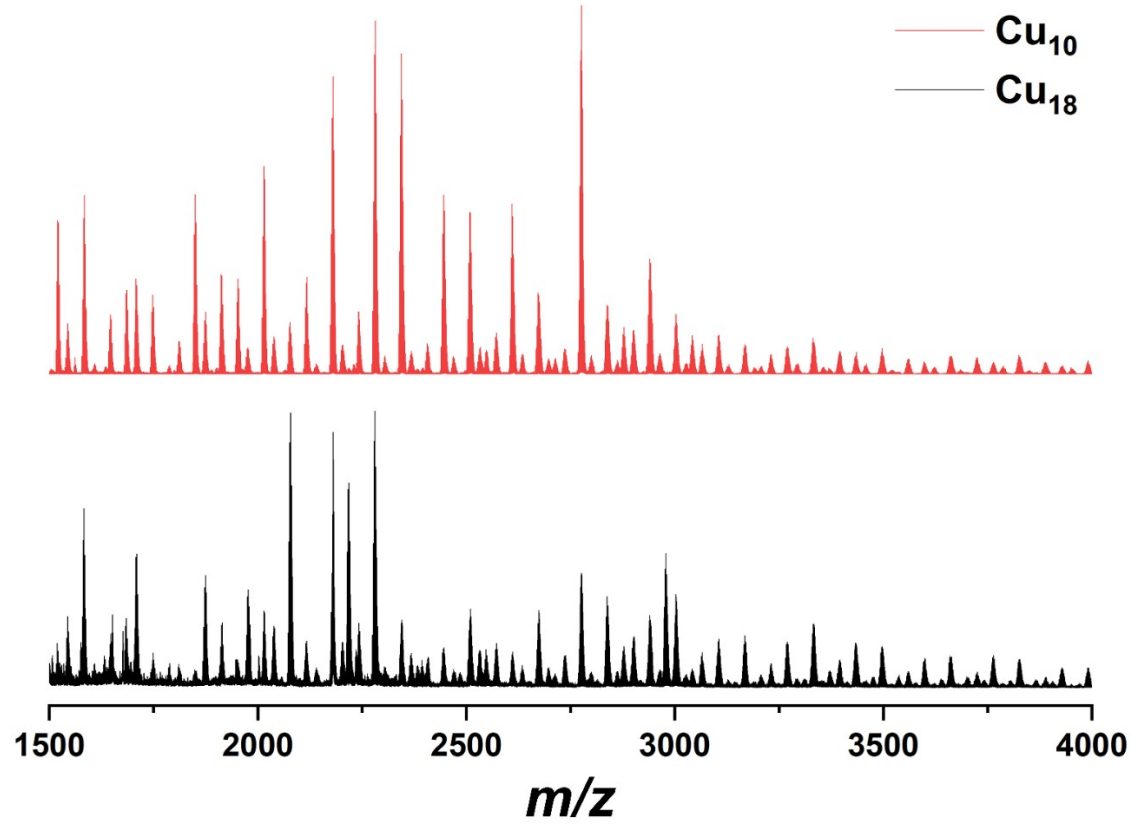

Fig. S8 Mass spectra (m/z range: 1500 – 4000) of (red) **Cu_{10}** and (black) **Cu_{18}.**

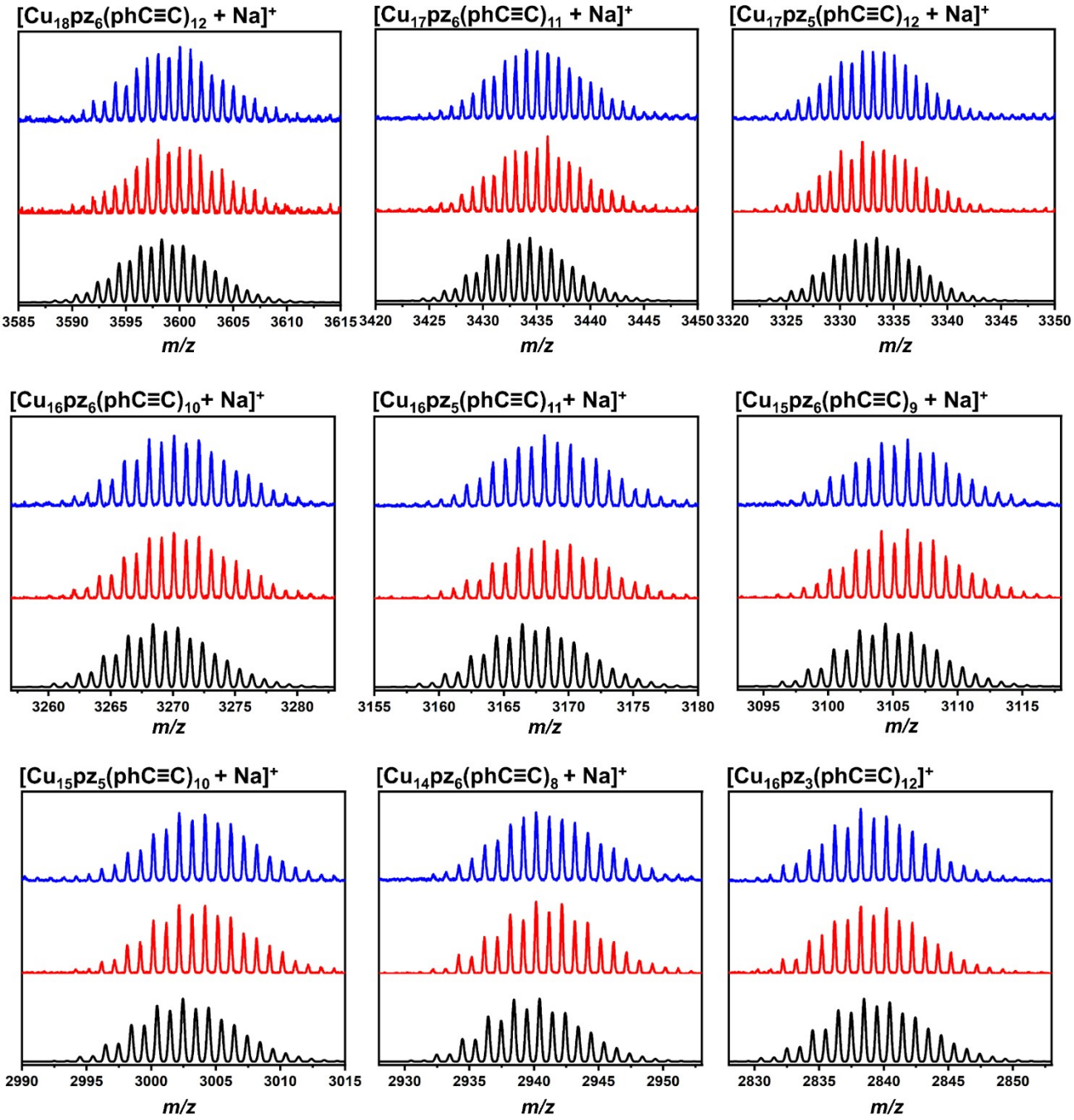
[Cu18pz6(phC≡C)12 + Na]+
3585 3590 3595 3600 3605 3610 3615
m/z
[Cu17pz6(phC≡C)11 + Na]+
3420 3425 3430 3435 3440 3445 3450
m/z
[Cu17pz5(phC≡C)12 + Na]+
3320 3325 3330 3335 3340 3345 3350
m/z
[Cu16pz6(phC≡C)10+ Na]+
3260 3265 3270 3275 3280
m/z
[Cu16pz5(phC≡C)11+ Na]+
3155 3160 3165 3170 3175 3180
m/z
[Cu15pz6(phC≡C)9 + Na]+
3095 3100 3105 3110 3115
m/z
[Cu15pz5(phC≡C)10 + Na]+
2990 2995 3000 3005 3010 3015
m/z
[Cu14pz6(phC≡C)8 + Na]+
2930 2935 2940 2945 2950
m/z
[Cu16pz3(phC≡C)12]+
2830 2835 2840 2845 2850
m/z

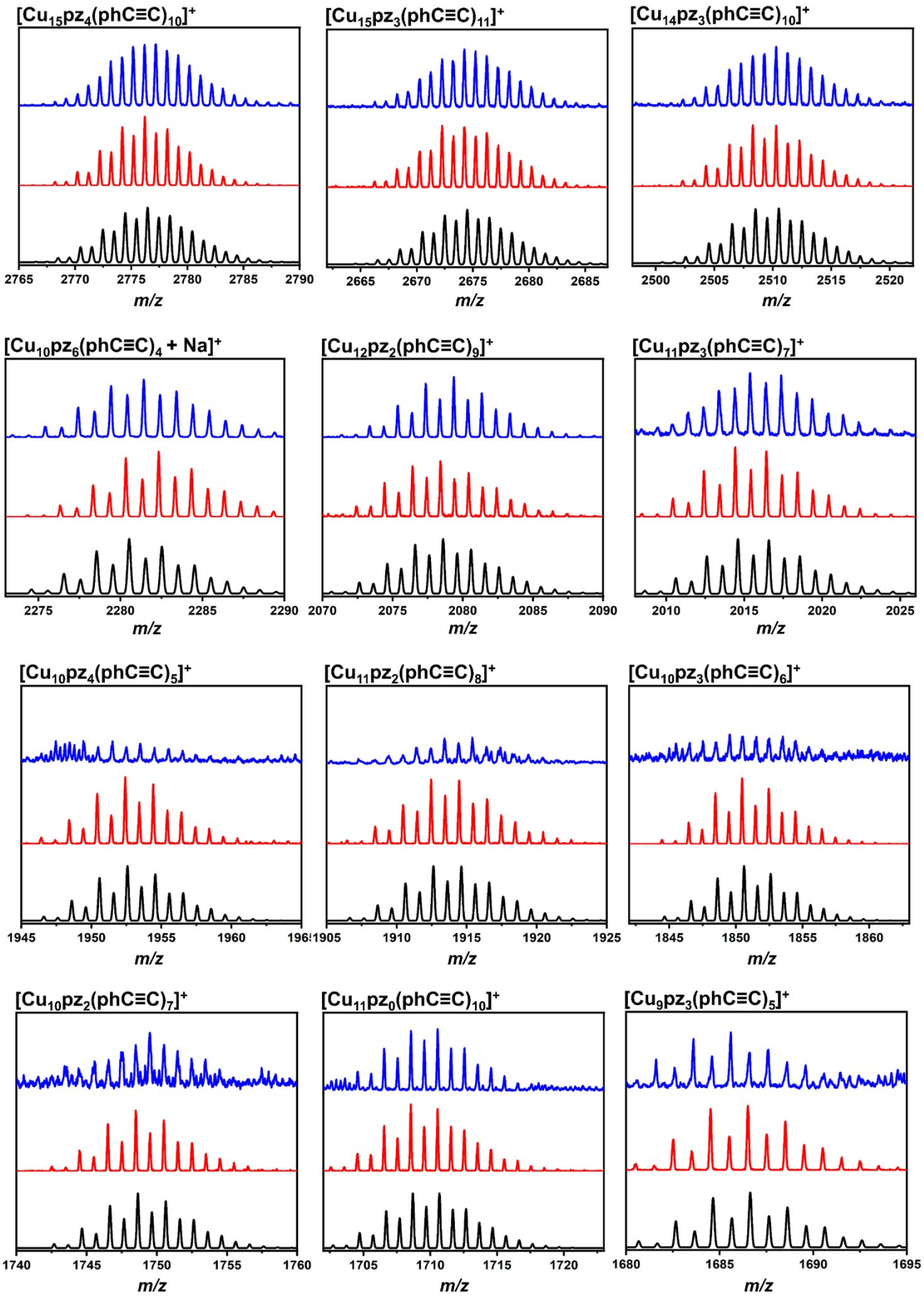
[Cu15pz4(phC≡C)10]+
2765 2770 2775 2780 2785 2790
m/z
[Cu15pz3(phC≡C)11]+
2665 2670 2675 2680 2685
m/z
[Cu14pz3(phC≡C)10]+
2500 2505 2510 2515 2520
m/z
[Cu10pz6(phC≡C)4 + Na]+
2275 2280 2285 2290
m/z
[Cu12pz2(phC≡C)9]+
2070 2075 2080 2085 2090
m/z
[Cu11pz3(phC≡C)7]+
2010 2015 2020 2025
m/z
[Cu10pz4(phC≡C)5]+
1945 1950 1955 1960
m/z
[Cu11pz2(phC≡C)8]+
1905 1910 1915 1920 1925
m/z
[Cu10pz3(phC≡C)6]+
1845 1850 1855 1860
m/z
[Cu10pz2(phC≡C)7]+
1740 1745 1750 1755 1760
m/z
[Cu11pz0(phC≡C)10]+
1705 1710 1715 1720
m/z
[Cu9pz3(phC≡C)5]+
1680 1685 1690 1695
m/z

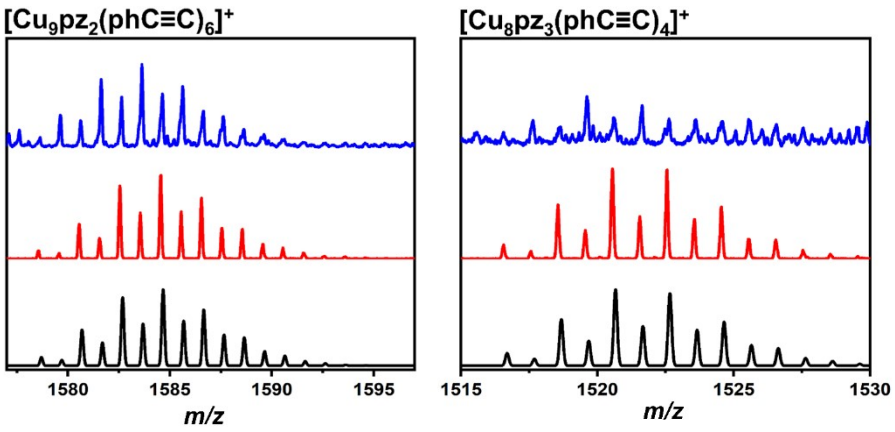

Fig. S9 Mass spectra of all nanoclusters corresponding to copper-containing species. Color representation: black, simulation; red, **Cu_{10}** and blue, **Cu_{18}.**

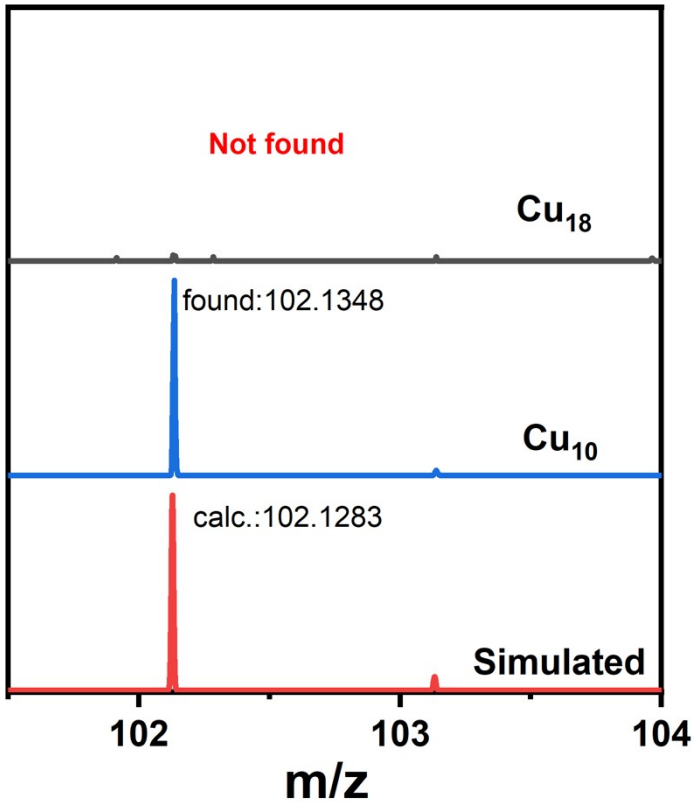

Fig. S10 Mass spectrum of counter cation (Et_3NH^+) of **Cu_{10}** and **Cu_{18}** in positive mode.

Note: Unfortunately, the monodispersed Cu alkyl cluster can't be observed in the test of the high-resolution mass spectrum due to them tend to dissociate, resulting in one set of fragment peaks. Therefore, only a series of heterogeneous peaks belonging to fragments are observed in the ESI-MS spectra of **Cu_{10}** and **Cu_{18}**.

PXRD

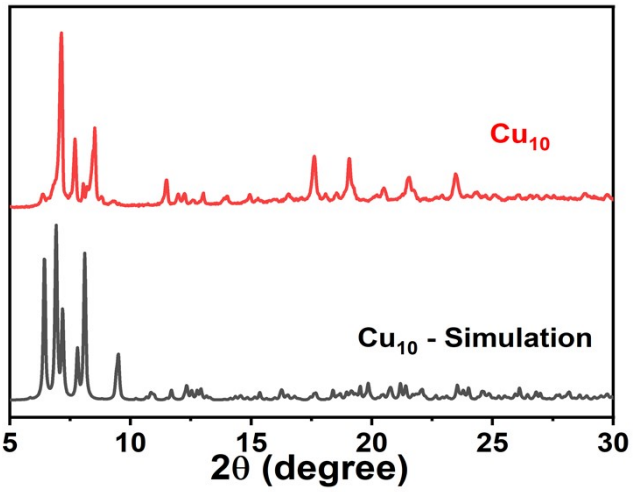

Fig. S11 Powder X-Ray Diffraction of experimental and simulation of **Cu_{10}**.

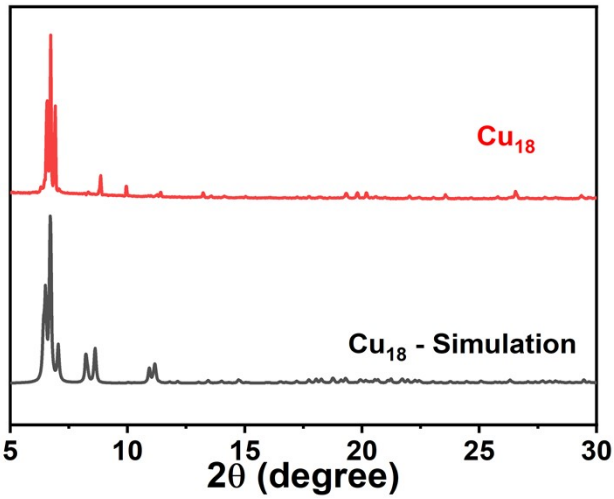

Fig. S12 Powder X-Ray Diffraction of experimental and simulation of **Cu_{18}**.

FT-IR

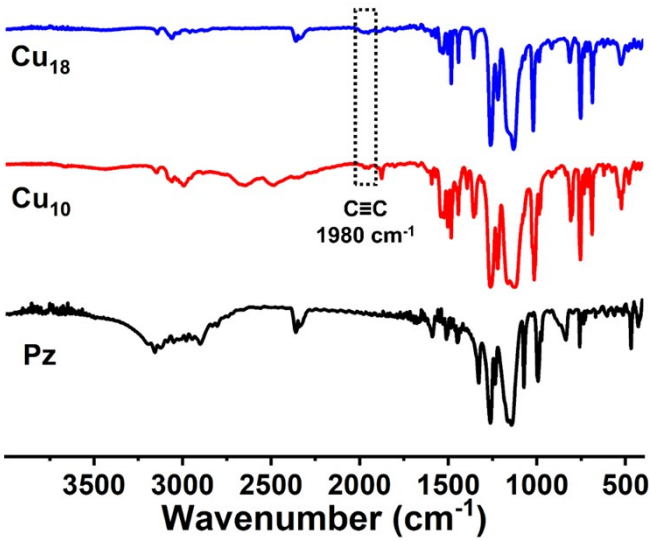

Fig. S13 FT-IR spectra of Pz, **Cu_{10}** and **Cu_{18}**.

XPS

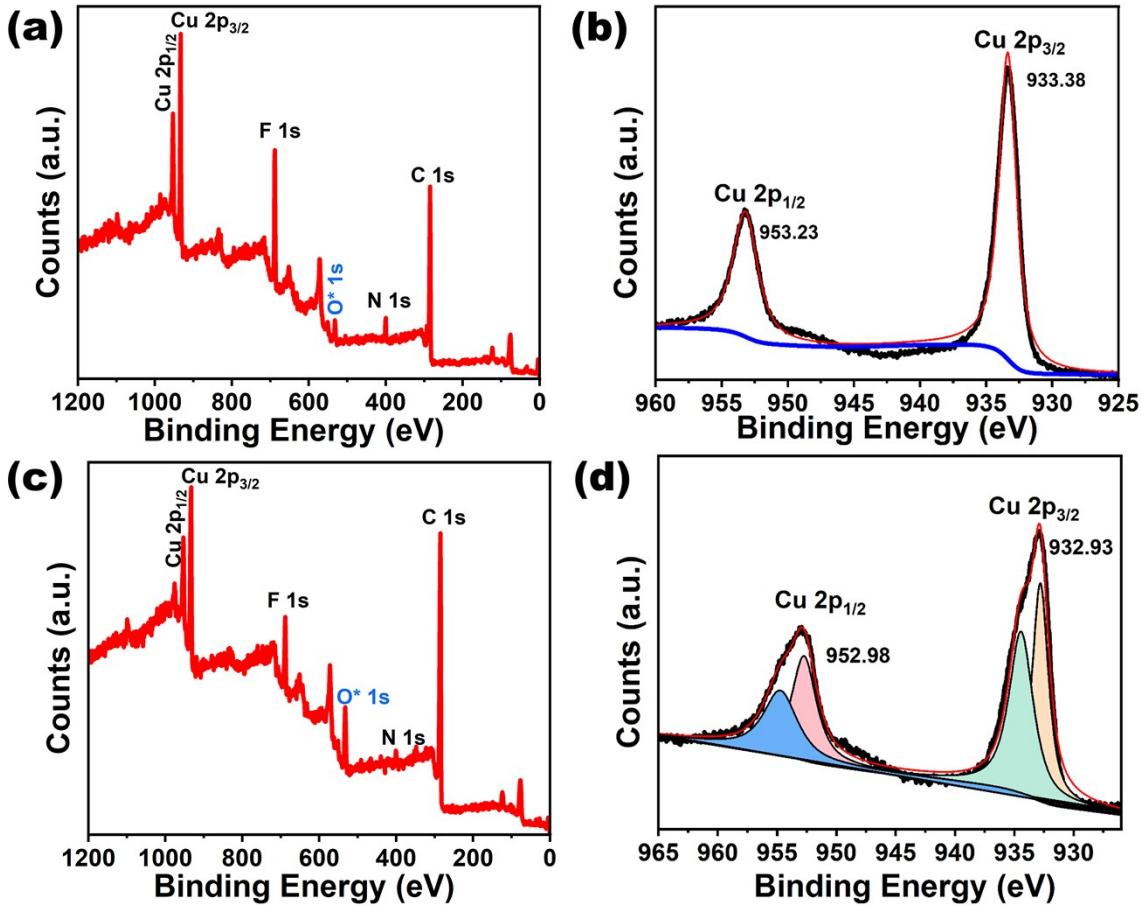

Fig. S14 XPS spectra of (a) **Cu_{10}** and (c) **Cu_{18},** XPS binding energies of copper regions for (b) **Cu_{10}** and (d) **Cu_{18}.**

Note: The alkynes in **Cu_{18}** exhibit a more complicated ligation mode compared to **Cu_{10}** (Fig. 2, Fig. 3), which results in multiple chemical environments of Cu(I), thus affecting the binding energy and inducing the minor split of peaks (Fig. S14d).

TGA

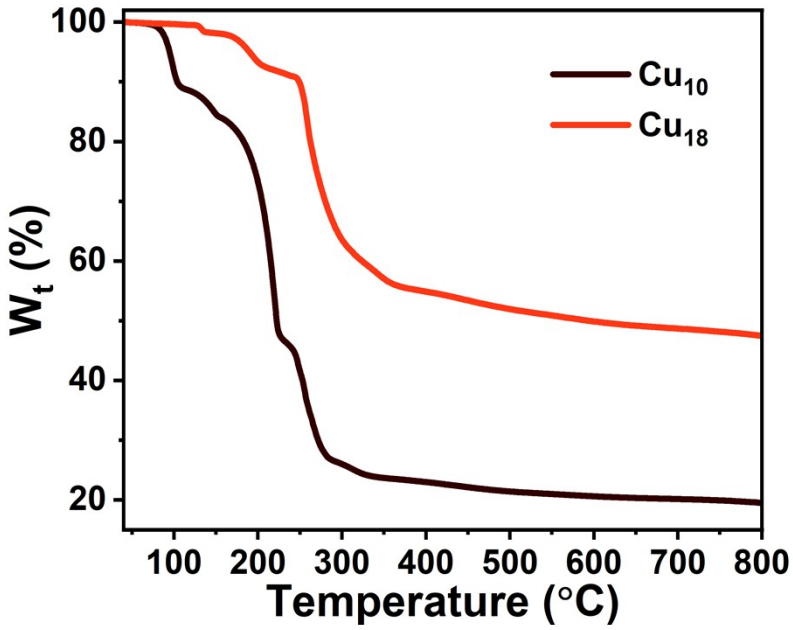

Fig. S15 Thermo gravimetric curves of **Cu_{10}** and **Cu_{18}**.

Photoluminescence data

Table S4 The photoluminescence photophyscial parameters of **Cu_{10}** and **Cu_{18}** in solid-state

Nanoclusters	T / K	λ_{abs}/nm	λ_{ex}/nm	λ_{em}/nm	τ_{av} / μs	Φ_{PL}	k_r/s^{-1}	k_{nr}/s^{-1}
Cu_{10}	300	317	400	514, 556, 695	8.4	0.35	4.17×10^4	7.74×10^4
	77			514, 565, 627	29.0			
Cu_{18}	300	348	500	620	2.8	0.63	2.25×10^5	1.32×10^5
	77			644	58.8			

Lifetime

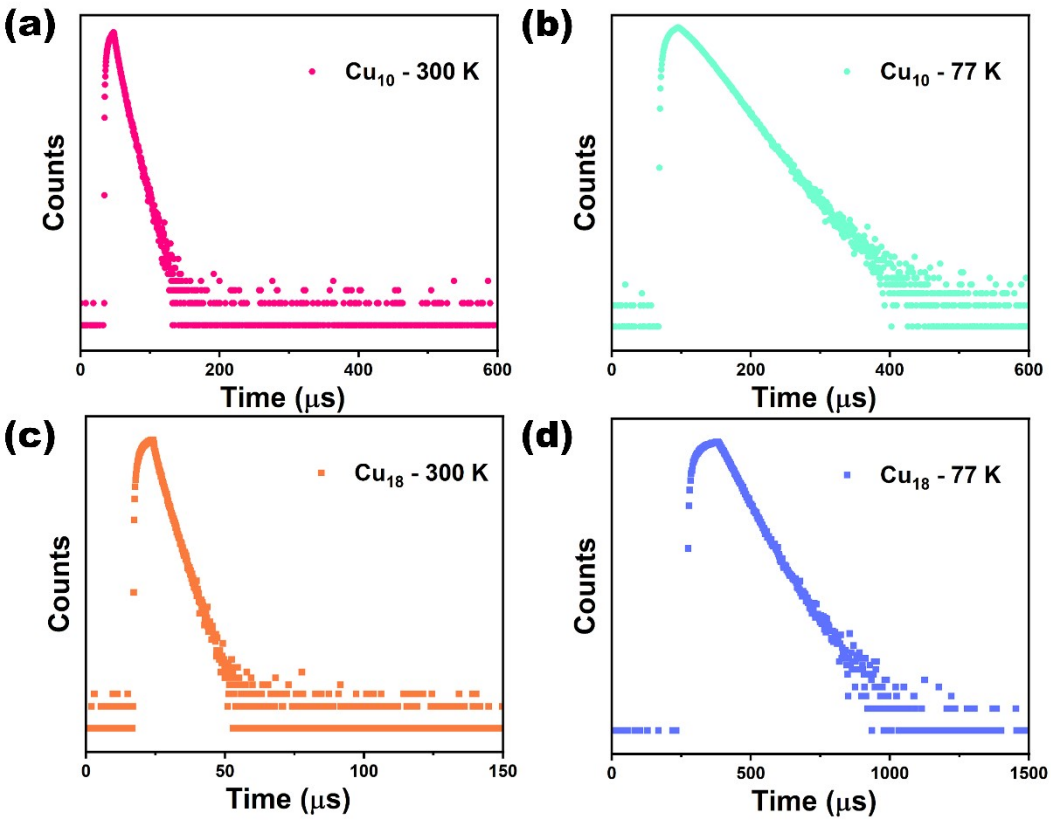

Fig. S16. Photoluminescence decay curve of (a) **Cu_{10}** and (c) **Cu_{18}** under 300 K and 77 K.

Table S5 Summary of photophysical parameters of all reported atomically precise CuNCs, including protected by S^-, P^-, I and $C\equiv C^-$ ligand.

Cu-cluster	Ligand	λ_{em} (nm)	PL QY	T[us]	*kr*(s^{-1})	ref.
$Cu_{24}S_{12}(PEt_2Ph)_{12}$	PEt_2Ph	680	0.390	1.45	2.69×10^5	5
$Cu_4I_4(PPh_2(CH_2)_2(CH_3)_2SiOSi\text{-}(CH_3)_2(CH_2)_2PPh_2)_2$		522	0.620	2.60	2.38×10^5	6
This work	Phenylacetylene, 3,5-$(CF_3)_2$Pz	620	0.630	2.80	2.25×10^5	
$Cu_4I_4(PPh_3)_4$	Triphenylphosphine	535	0.910	4.20	2.17×10^5	7
$Cu_6I_6(PPh_2(CH_2)_3PPh_2)_3$	1,3-bis(diphenylphosphino)propane	655	0.390	2.125	1.84×10^5	7
$[Cu_{11}(TBBT)_9(PPh_3)_6](SbF_6)_2$	4-tert-butylbenzenethiol	675	0.220	1.30	1.69×10^5	8
$Cu_4I_4(PPh_2(CH_2)_2(CH_3)_2SiOSi\text{-}(CH_3)_2(CH_2)_2PPh_2)_3$		571	0.670	6.10	1.10×10^5	6
$Cu_{12}S_6(dppo)_4$	dppo =$Ph_2P(CH_2)_8PPh_2$	665	0.670	6.50	1.03×10^5	9
$Cu_{12}Se_6(dppo)_4$	dppo =$Ph_2P(CH_2)_8PPh_2$	638	0.530	5.26	1.01×10^5	5
$Cu_{10}(12\text{-}C\equiv C\text{-}closo\text{-}CB_{11}H_{11})_5(4\text{-}CH_3Py)_9$	12-C≡C-closo-$CB_{11}H_{21}$	670	0.560	6.37	8.79×10^4	10
$Cu_8(12\text{-}C\equiv C\text{-}closo\text{-}CB_{11}H_{11})4(3\text{-}CH_3Py)_8(NH_3)$	12-C≡C-closo-$CB_{11}H_{20}$	660	0.460	5.83	7.89×10^4	10
$Cu_{12}S_6(dpppt)_4$	dpppt =$Ph_2P(CH_2)_5PPh_2$	648	0.480	6.10	7.87×10^4	9
$Cu_{14}(C_2B_{10}H_{10}S_2)_6(CH_3CN)_8$	$C_2B_{10}H_{10}S_2H$	637, 661	0.310	5.13	6.04×10^4	11
$[Cu_4(PCP)_3][BF_4]$	PCP = 2,6-$(PPh_2)_2C_6H_3$	518	0.500	9.800	5.10×10^4	12
This work	Phenylacetylene, 3,5-$(CF_3)_2$Pz	514, 556	0.350	8.40	4.17×10^4	
$[Cu_6(C_2C_6H_4NMe_2)_4\{(PPh_2)_3CH\}_2](PF_6)_2$	C_2-4-C_6H_4-NMe_2	658	0.015	0.447	3.36×10^4	13
$Cu_8(12\text{-}C\equiv C\text{-}closo\text{-}CB_{11}H_{11})_4(Py)_8$	12-C≡C-closo-$CB_{11}H_{19}$	650	0.130	5.43	2.39×10^4	10
$[(TripC\equiv C)Cu]_8$	2,4,6-iPr_3-C_6H_2	599	0.210	10.40	2.02×10^4	14
$Cu(3,5\text{-lutidine})_4][Cu_7(12\text{-}C\equiv C\text{-}closo\text{-}CB_{11}H_{11})_4(3,5\text{-lutidine})_8$	12-C≡C-closo-$CB_{11}H_{18}$	580	0.100	5.24	1.91×10^4	10
$[Cu_6(C_2Ph)_4\{(PPh_2)_3CH\}_2](PF_6)_2$	C_2-4-C_6H_5	615	0.165	11.48	1.44×10^4	13
$Cu_4(12\text{-}C\equiv C\text{-}closo\text{-}CB_{11}H_{11})_2(PPh_3)_4$	12-C≡C-closo-$CB_{11}H_{16}$	494	0.990	75.64	1.31×10^4	10
$[Cu_6(C_2C_6H_4OMe)_4\{(PPh_2)_3CH\}_2](PF_6)_2$	C_2-4-C_6H_4-OMe	621	0.041	3.175	1.29×10^4	13
$[Cu_6(C_2C_6H_4Ph)_4\{(PPh_2)_3CH\}_2](PF_6)_2$	C_2-4-C_6H_4-Ph	624	0.075	6.80	1.10×10^4	13
$Cu(PPh)_3][Cu_3(12\text{-}C\equiv C\text{-}closo\text{-}CB_{11}H_{11})_2(PPh_3)_4$	12-C≡C-closo-$CB_{11}H_{15}$	490	0.570	51.95	1.10×10^4	10
$Cu_4(12\text{-}C\equiv C\text{-}closo\text{-}CB_{11}H_{11})_2(PiPr3)_4$	12-C≡C-closo-$CB_{11}H_{12}$	512	0.990	98.00	1.01×10^4	10
$[Cu_6(C_2C_5H_4N)_4\{(PPh_2)_3CH\}_2](PF_6)_2$	$C_2C_5H_4N$	508	0.037	4.695	7.88×10^3	13
$Cu_4(12\text{-}C\equiv C\text{-}closo\text{-}CB_{11}H_{11})_2(PCy_3)$	12-C≡C-closo-$CB_{11}H_{14}$	509	0.800	105.20	7.60×10^3	10
$[Cu_6(C_2C_6H_4CF_3)_4\{(PPh_2)_3CH\}_2](PF_6)_2$	C_2-4-C_6H_4-CF_3	579	0.117	17.80	6.57×10^3	13
$Cu(PMe_3)_4]_2[Cu_6(12\text{-}C\equiv C\text{-}closo\text{-}CB_{11}H_{11})4(PMe_3)_5$	12-C≡C-closo-$CB_{11}H_{17}$	640	0.030	7.00	4.29×10^3	10
R/S-Cu_{14}	(R/S)-2diphenyl-2-hydroxylmethylpyrrolidine-1-propyne	726	0.082	61.15	1.34×10^3	15
Cu_3I_6	non	548	0.120	1580	7.59	16

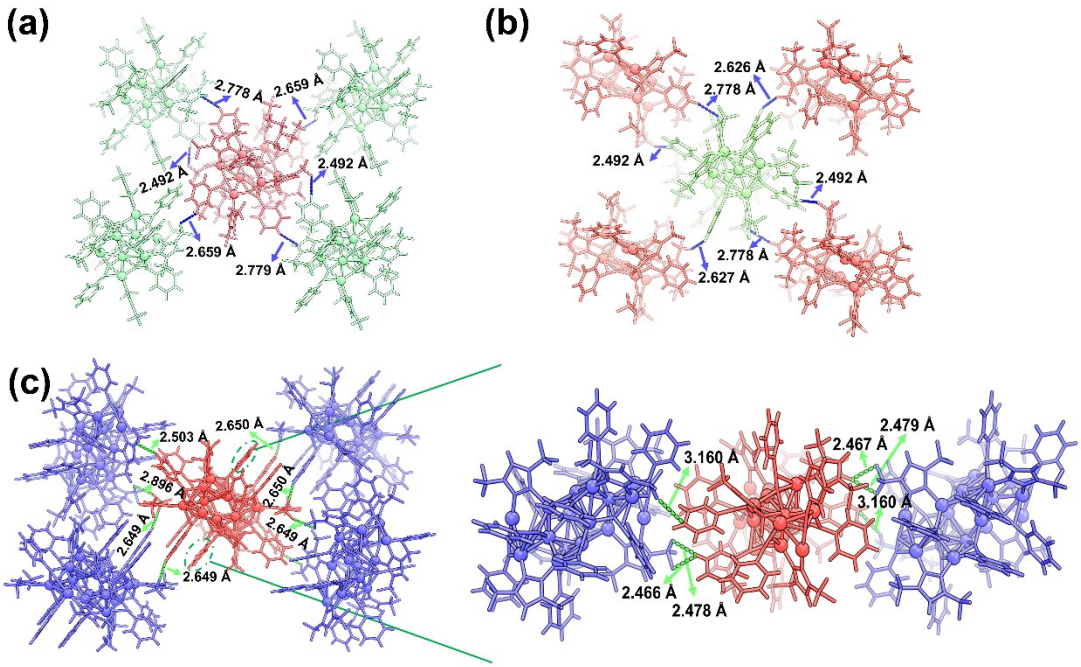

Fig. S17 Hydrogen bonding interactions in **Cu_{10}-a** (a), **Cu_{10}-b (b)**, and **Cu_{18}** (c) (d).

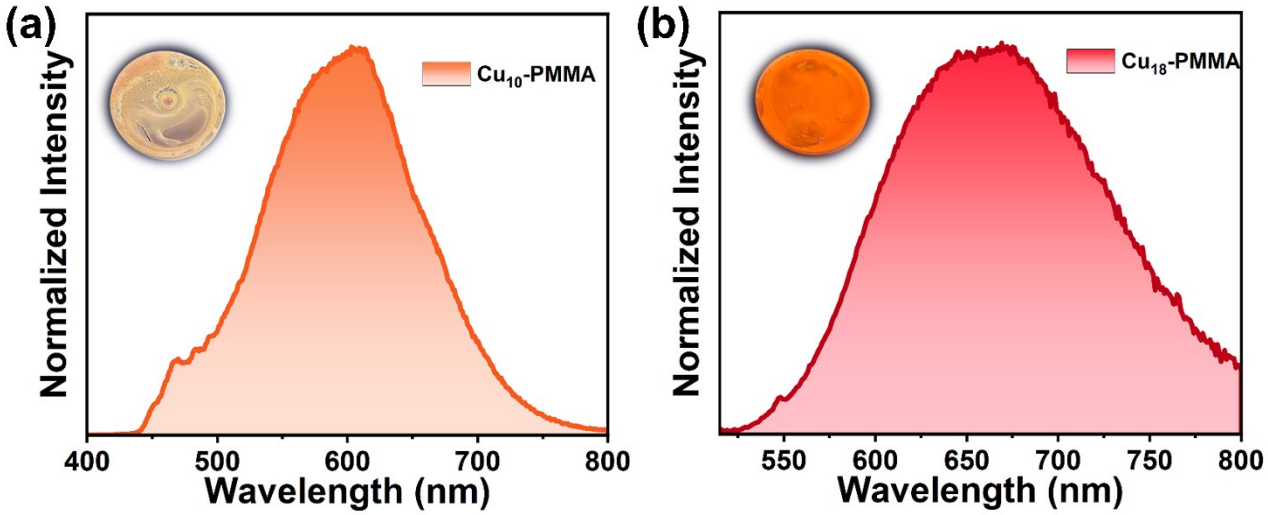

Fig. S18 Solid-state emission of polymethyl methacrylate film with 15% weight of **Cu_{10}** (a) and **Cu_{18}** (b).

Computational detail

To figure out the absorption and emission, density functional theory (DFT) and time-dependent DFT (TD-DFT) were performed. For detail, geometry optimization at the ground state was carried out by DFT utilizing the AMS2018 program[17, 18] with the B3LYP-DJ[19] function and triple zeta polarization (TZP) basis set.[20] Crystal structures were used as the initial guess for geometry optimization. Kohn-Sham orbitals were obtained by Gaussian16 package[21] under the level of PBE function in conjunction with Def2-SVP basis set,[22] and their maps and population analysis were conducted by Multiwfn 3.8,[23] followed by visualized via VMD 1.9.3 program.[24] To assign the electronic transition, TD-DFT was performed through the AMS2018 program and the first 1500 singlets of optimized geometry (S_0) were calculated using TD-DFT+TB (tight-binding) formalism for linear response, to simulate absorption spectra at an affordable computational cost.[25] All the calculations in the AMS2018 program are treated with ZORA Hamiltonian for scalar relativistic effects.[26-28]

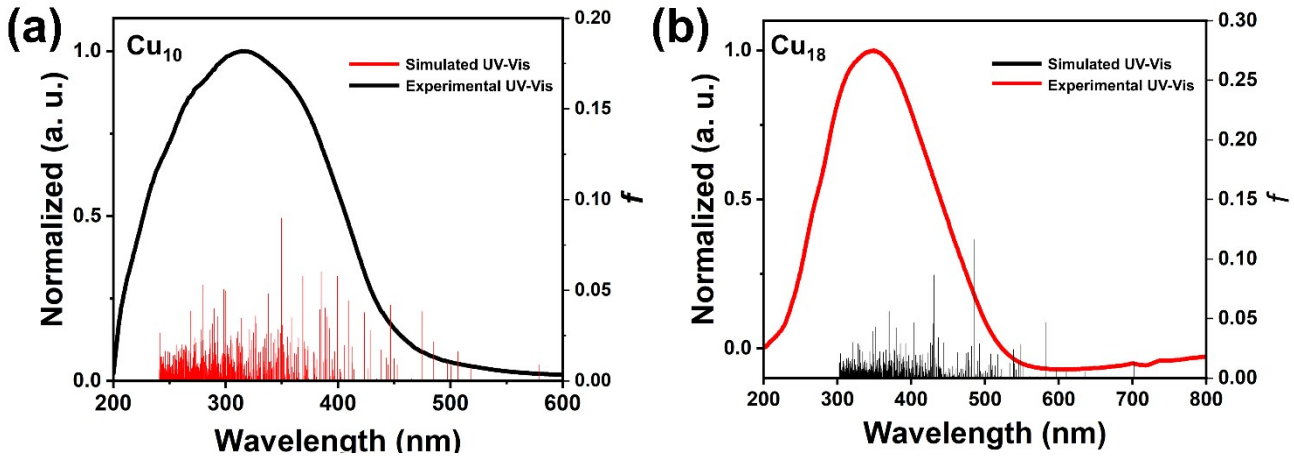

Fig. S19 The comparison between experimental solid-state UV-vis spectra with simulated UV-vis of **Cu_{10}** (a) and **Cu_{18}** (b).

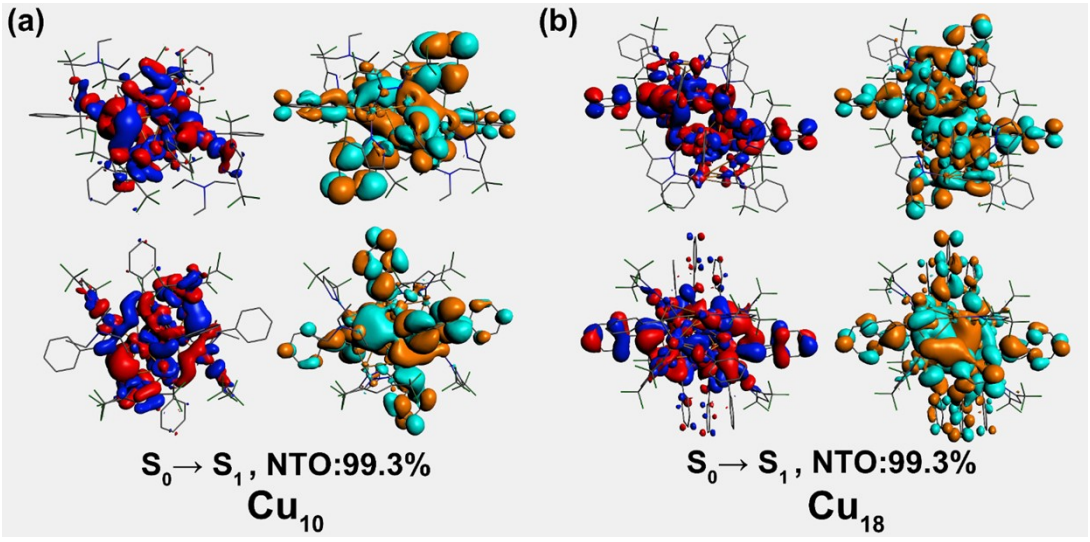

Fig. S20 Natural transition orbitals (NTOs) for S_0 to S_1 of **Cu_{10}** (a) **and Cu_{18}** (b) (isovalue = 0.01 a.u., upper: side view, bottom: top view).

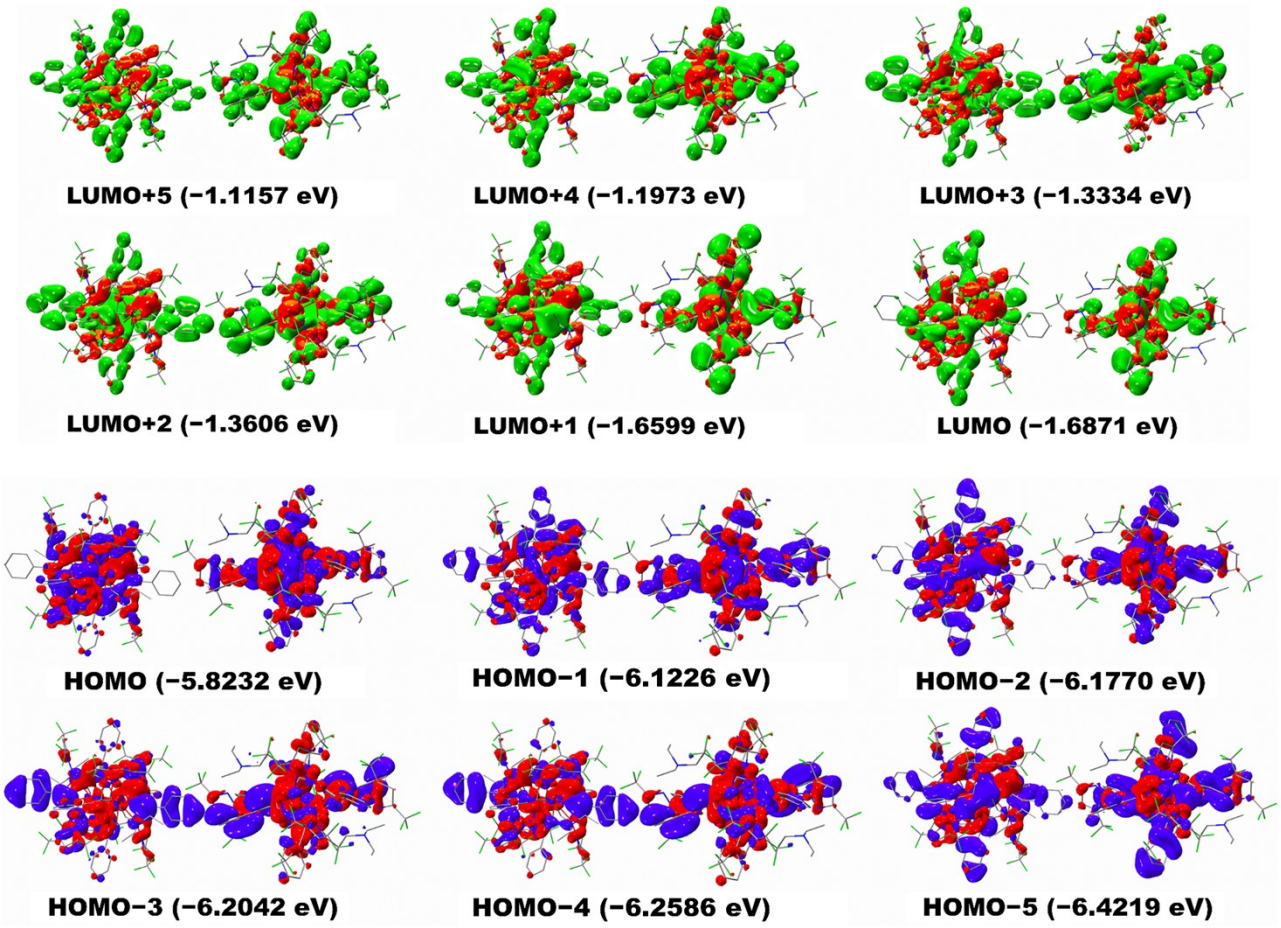

Fig. S21. Frontier molecular orbitals of $\mathbf{Cu_{10}}$ (isovalue = 0.01 a.u., left: side view, right: top view).

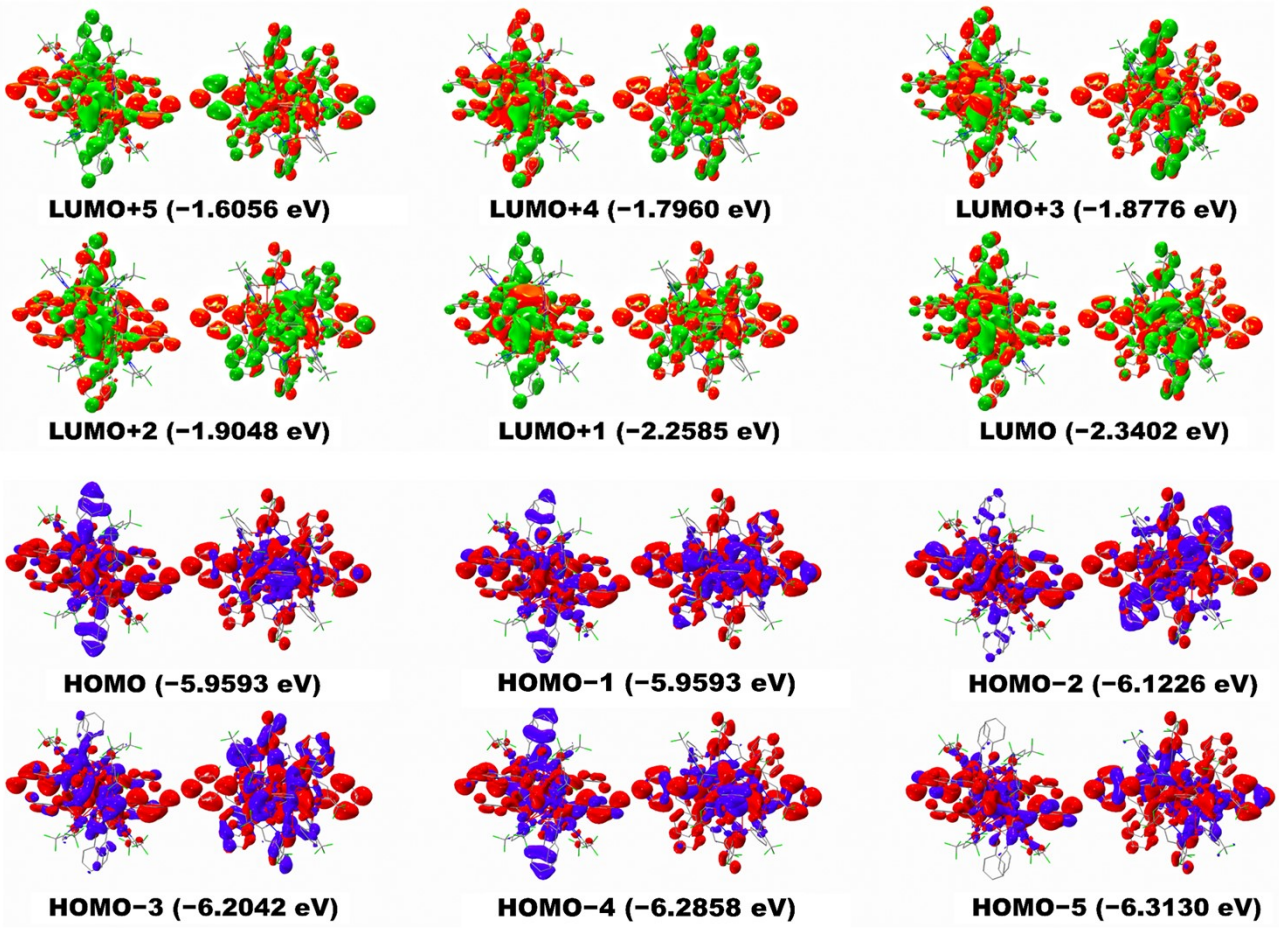

Fig. S22. Frontier molecular orbitals of $\mathbf{Cu_{18}}$ (isovalue = 0.01 a.u., left: side view, right: top view).

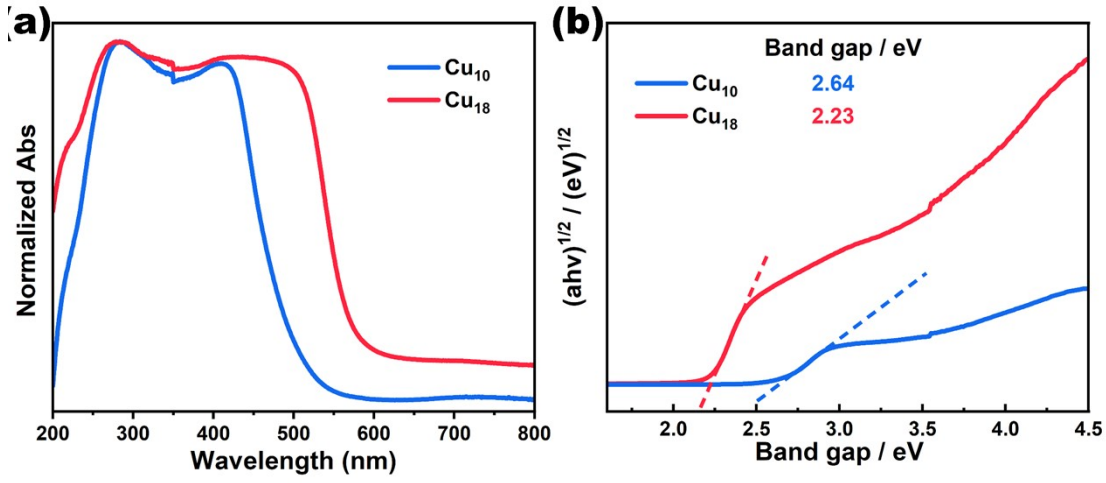

Fig. S23. Solid-state V-Vis diffuse reflectance spectroscopies (a) and corresponding band gaps (b) of $\mathbf{Cu_{10}}$ and $\mathbf{Cu_{18}}$.

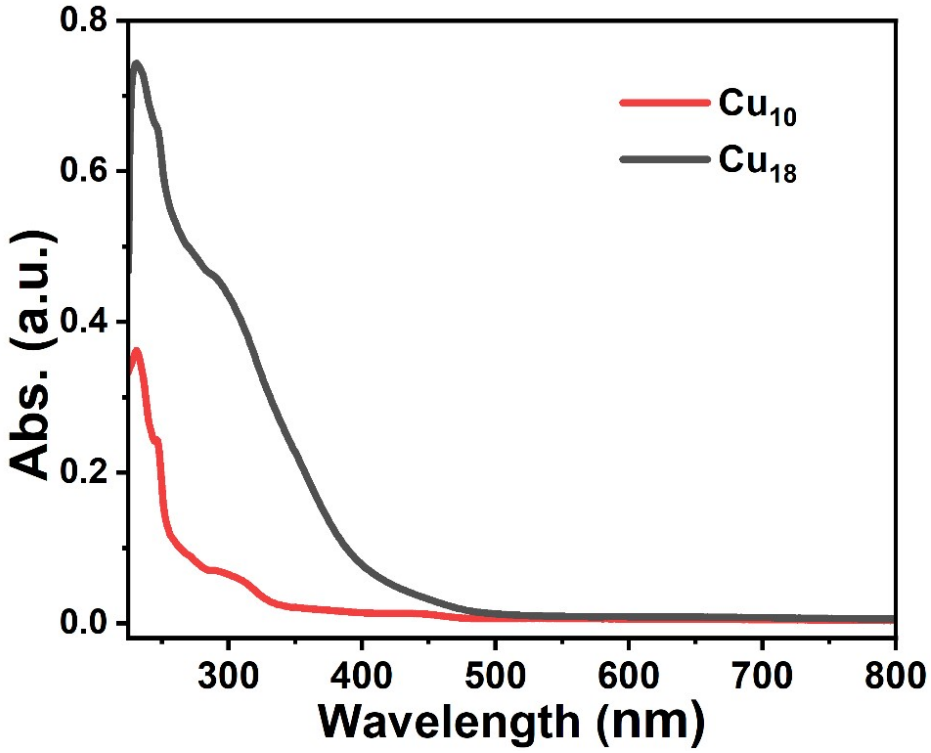

Fig. S24. The UV-vis spectra of **Cu_{10}** and **Cu_{18}** in CH_2Cl_2 (cluster concentration:6.7×10^{-6} mol L^{-1}).

Table S6. Selected bond length (Å) and bond angles (°) of **Cu_{10}**.

Cu(7)-Cu(6)	3.0361(14)	Cu(3)-N(2)	1.996(6)	Cu(1)-C(39)#2	2.124(7)
Cu(8)-Cu(9)#1	2.9964(14)	Cu(7)-N(9)	1.994(6)	Cu(1)-C(31)#2	2.118(7)
Cu(9)-Cu(6)	2.9790(13)	Cu(7)-N(8)	1.988(5)	Cu(6)-C(76)#1	2.118(6)
Cu(4)-Cu(2)#2	2.9667(14)	Cu(8)-N(10)	1.984(6)	Cu(8)-C(84)#1	2.080(7)
Cu(3)-Cu(2)	2.9515(13)	Cu(3)-N(4)	1.984(6)	Cu(2)-C(38)#2	2.078(7)
Cu(9)-Cu(9)#1	2.9423(19)	Cu(2)-N(3)	1.973(6)	Cu(2)-C(39)#2	2.077(6)
Cu(8)-Cu(7)	2.9102(13)	Cu(6)-N(7)	1.971(6)	Cu(5)-C(22)	2.074(7)
Cu(8)-Cu(6)	2.7406(14)	Cu(1)-N(1)	1.962(6)	Cu(2)-C(31)	2.068(7)
Cu(4)-Cu(2)	2.7318(13)	Cu(10)-N(12)	1.939(6)	Cu(8)-C(83)#1	2.053(6)
Cu(9)-Cu(6)#1	2.7138(13)	Cu(5)-N(5)	1.934(6)	Cu(8)-C(76)	2.046(6)
Cu(1)-Cu(4)#2	2.7026(14)	Cu(1)-C(30)#2	2.297(7)	Cu(10)-C(67)	2.029(6)
Cu(8)-Cu(9)	2.6990(13)	Cu(6)-C(83)#1	2.241(7)	Cu(5)-C(23)	2.027(7)
Cu(9)-Cu(7)	2.6850(14)	Cu(4)-C(39)	2.209(7)	Cu(9)-C(68)	2.017(7)
Cu(3)-Cu(4)	2.6754(14)	Cu(9)-C(84)	2.196(7)	Cu(4)-C(23)	2.013(7)
Cu(1)-Cu(2)	2.6706(14)	Cu(6)-C(75)#1	2.189(7)	Cu(10)-C(68)	2.013(6)
Cu(5)-Cu(4)	2.5029(13)	Cu(6)-C(84)#1	2.170(7)	Cu(5)-C(39)	1.996(6)
Cu(9)-C(76)	1.988(6)	Cu(10)-C(84)	1.985(7)	Cu(4)-C(31)	1.979(7)
Cu(3)-C(23)	1.974(7)	Cu(7)-C(68)	1.955(6)	CA8:A59(23)-Cu(4)-Cu(2)	113.2(2)
Cu(1)#2-Cu(4)-Cu(2)	97.02(4)	N(1)-Cu(1)-C(30)#2	95.2(2)	C(23)-Cu(4)-Cu(2)#2	119.6(2)
Cu(1)#2-Cu(4)-Cu(2)#2	55.97(3)	N(1)-Cu(1)-C(31)#2	126.2(3)	C(23)-Cu(4)-Cu(3)	47.2(2)
Cu(1)-Cu(2)-Cu(3)	67.63(4)	N(1)-Cu(1)-C(38)#2	100.6(3)	C(23)-Cu(4)-Cu(5)	52.0(2)
Cu(1)-Cu(2)-Cu(4)	71.78(4)	N(1)-Cu(1)-C(39)#2	134.7(3)	C(23)-Cu(5)-C(22)	35.3(3)

Cu(1)-Cu(2)-Cu(4)#2	57.00(3)	N(1)-Cu(1)-Cu(2)	113.89(18)	C(23)-Cu(5)-Cu(4)	51.47(19)
Cu(10)-Cu(9)-Cu(6)	127.14(5)	N(1)-Cu(1)-Cu(4)#2	171.54(18)	C(30)#2-Cu(1)-Cu(2)	124.93(18)
Cu(10)-Cu(9)-Cu(6)#1	96.66(4)	N(10)-Cu(8)-C(83)#1	113.8(3)	C(30)#2-Cu(1)-Cu(4)#2	78.14(18)
Cu(10)-Cu(9)-Cu(7)	97.80(4)	N(10)-Cu(8)-C(84)#1	148.4(3)	C(31)#2-Cu(1)-C(30)#2	31.9(3)
Cu(10)-Cu(9)-Cu(8)	159.90(5)	N(10)-Cu(8)-Cu(6)	126.69(17)	C(31)#2-Cu(1)-C(38)#2	132.9(3)
Cu(10)-Cu(9)-Cu(8)#1	81.92(4)	N(10)-Cu(8)-Cu(7)	66.76(16)	C(31)#2-Cu(1)-C(39)#2	99.1(3)
Cu(10)-Cu(9)-Cu(9)#1	135.91(6)	N(10)-Cu(8)-Cu(9)	103.87(17)	C(31)#2-Cu(1)-Cu(2)	99.83(19)
Cu(2)-Cu(1)-Cu(4)#2	67.02(4)	N(10)-Cu(8)-Cu(9)#1	164.28(17)	C(31)#2-Cu(1)-Cu(4)#2	46.54(18)
Cu(2)-Cu(4)-Cu(2)#2	113.13(4)	N(12)-Cu(10)-C(67)	111.3(3)	C(31)-Cu(2)-C(38)#2	144.2(3)
Cu(3)-Cu(2)-Cu(4)#2	109.19(4)	N(12)-Cu(10)-C(68)	146.6(3)	C(31)-Cu(2)-C(39)#2	109.0(3)
Cu(3)-Cu(4)-Cu(1)#2	159.67(5)	N(12)-Cu(10)-C(84)	104.3(3)	C(31)-Cu(2)-Cu(1)	105.78(19)
Cu(3)-Cu(4)-Cu(2)	66.16(4)	N(12)-Cu(10)-Cu(9)	156.19(18)	C(31)-Cu(2)-Cu(3)	97.43(18)
Cu(3)-Cu(4)-Cu(2)#2	139.80(5)	N(2)-Cu(3)-Cu(2)	107.12(17)	C(31)-Cu(2)-Cu(4)	46.18(18)
Cu(4)-Cu(2)-Cu(3)	56.00(3)	N(2)-Cu(3)-Cu(4)	117.94(17)	C(31)-Cu(2)-Cu(4)#2	63.17(19)
Cu(4)-Cu(2)-Cu(4)#2	66.87(4)	N(3)-Cu(2)-C(31)	107.2(3)	C(31)-Cu(4)-C(23)	146.1(3)
Cu(4)-Cu(3)-Cu(2)	57.84(3)	N(3)-Cu(2)-C(38)#2	108.7(3)	C(31)-Cu(4)-C(39)	100.7(3)
Cu(5)-Cu(4)-Cu(1)#2	95.69(4)	N(3)-Cu(2)-C(39)#2	142.6(3)	C(31)-Cu(4)-Cu(1)#2	51.0(2)
Cu(5)-Cu(4)-Cu(2)	163.62(5)	N(3)-Cu(2)-Cu(1)	125.23(18)	C(31)-Cu(4)-Cu(2)	48.9(2)
Cu(5)-Cu(4)-Cu(2)#2	82.63(4)	N(3)-Cu(2)-Cu(3)	65.74(17)	C(31)-Cu(4)-Cu(2)#2	94.1(2)
Cu(5)-Cu(4)-Cu(3)	99.15(4)	N(3)-Cu(2)-Cu(4)	103.05(17)	C(31)-Cu(4)-Cu(3)	109.2(2)
Cu(6)#1-Cu(9)-Cu(6)	117.97(4)	N(3)-Cu(2)-Cu(4)#2	169.12(18)	C(31)-Cu(4)-Cu(5)	138.0(2)
Cu(6)#1-Cu(9)-Cu(8)#1	57.10(3)	N(4)-Cu(3)-Cu(2)	66.84(16)	C(38)#2-Cu(1)-C(30)#2	164.1(3)
Cu(6)#1-Cu(9)-Cu(9)#1	63.41(4)	N(4)-Cu(3)-Cu(4)	102.63(18)	C(38)#2-Cu(1)-Cu(2)	49.57(18)
Cu(6)-Cu(8)-Cu(7)	64.92(3)	N(4)-Cu(3)-N(2)	127.4(3)	C(38)#2-Cu(1)-Cu(4)#2	86.35(19)
Cu(6)-Cu(8)-Cu(9)#1	56.25(3)	N(5)-Cu(5)-C(22)	111.2(3)	C(38)#2-Cu(2)-Cu(1)	52.43(18)
Cu(6)-Cu(9)-Cu(8)#1	85.12(4)	N(5)-Cu(5)-C(23)	145.6(3)	C(38)#2-Cu(2)-Cu(3)	98.12(18)
Cu(7)-Cu(8)-Cu(9)#1	106.83(4)	N(5)-Cu(5)-C(39)	105.1(3)	C(38)#2-Cu(2)-Cu(4)	124.20(19)
Cu(7)-Cu(9)-Cu(6)	64.59(3)	N(5)-Cu(5)-Cu(4)	157.65(18)	C(38)#2-Cu(2)-Cu(4)#2	81.24(19)
Cu(7)-Cu(9)-Cu(6)#1	157.86(5)	N(7)-Cu(6)-C(75)#1	103.0(2)	C(39)#2-Cu(1)-C(30)#2	129.6(3)
Cu(7)-Cu(9)-Cu(8)	65.44(4)	N(7)-Cu(6)-C(76)#1	135.7(2)	C(39)#2-Cu(1)-C(38)#2	34.5(3)
Cu(7)-Cu(9)-Cu(8)#1	141.87(5)	N(7)-Cu(6)-C(83)#1	93.3(2)	C(39)#2-Cu(1)-Cu(2)	49.76(18)
Cu(7)-Cu(9)-Cu(9)#1	114.82(5)	N(7)-Cu(6)-C(84)#1	126.3(2)	C(39)#2-Cu(1)-Cu(4)#2	52.84(19)
Cu(8)-Cu(6)-Cu(7)	60.24(3)	N(7)-Cu(6)-Cu(7)	64.51(17)	C(39)#2-Cu(2)-C(38)#2	35.6(3)
Cu(8)-Cu(6)-Cu(9)	56.13(3)	N(7)-Cu(6)-Cu(8)	108.66(18)	C(39)#2-Cu(2)-Cu(1)	51.30(18)
Cu(8)-Cu(7)-Cu(6)	54.84(3)	N(7)-Cu(6)-Cu(9)	114.47(17)	C(39)#2-Cu(2)-Cu(3)	117.60(19)
Cu(8)-Cu(9)-Cu(6)	57.47(3)	N(7)-Cu(6)-Cu(9)#1	175.09(18)	C(39)#2-Cu(2)-Cu(4)	108.47(19)
Cu(8)-Cu(9)-Cu(6)#1	96.61(4)	N(8)-Cu(7)-Cu(6)	64.76(16)	C(39)#2-Cu(2)-Cu(4)#2	48.06(19)
Cu(8)-Cu(9)-Cu(8)#1	118.05(4)	N(8)-Cu(7)-Cu(8)	102.72(16)	C(39)-Cu(4)-Cu(1)#2	50.00(17)
Cu(8)-Cu(9)-Cu(9)#1	64.00(4)	N(8)-Cu(7)-Cu(9)	124.65(17)	C(39)-Cu(4)-Cu(2)	145.64(17)
Cu(9)#1-Cu(6)-Cu(7)	111.04(4)	N(8)-Cu(7)-N(9)	117.7(2)	C(39)-Cu(4)-Cu(2)#2	44.39(16)
Cu(9)#1-Cu(6)-Cu(8)	66.64(4)	N(9)-Cu(7)-Cu(6)	119.34(16)	C(39)-Cu(4)-Cu(3)	148.14(17)
Cu(9)#1-Cu(6)-Cu(9)	62.04(4)	N(9)-Cu(7)-Cu(8)	67.22(16)	C(39)-Cu(4)-Cu(5)	49.65(16)
Cu(9)#1-Cu(9)-Cu(6)	54.55(3)	N(9)-Cu(7)-Cu(9)	101.67(16)	C(39)-Cu(5)-C(22)	143.6(3)
Cu(9)#1-Cu(9)-Cu(8)#1	54.05(4)	C(22)-Cu(5)-Cu(4)	86.73(19)	C(39)-Cu(5)-C(23)	108.4(3)

Cu(9)-Cu(6)-Cu(7)	53.01(3)	C(23)-Cu(3)-Cu(2)	106.2(2)	C(39)-Cu(5)-Cu(4)	57.50(19)
Cu(9)-Cu(7)-Cu(6)	62.40(3)	C(23)-Cu(3)-Cu(4)	48.5(2)	C(67)-Cu(10)-Cu(9)	88.08(18)
Cu(9)-Cu(7)-Cu(8)	57.51(3)	C(23)-Cu(3)-N(2)	109.3(3)	C(68)-Cu(10)-C(67)	36.3(3)
Cu(9)-Cu(8)-Cu(6)	66.41(4)	C(23)-Cu(3)-N(4)	122.8(3)	C(68)-Cu(10)-Cu(9)	51.89(19)
Cu(9)-Cu(8)-Cu(7)	57.05(3)	C(23)-Cu(4)-C(39)	101.1(3)	C(68)-Cu(7)-Cu(6)	91.33(19)
Cu(9)-Cu(8)-Cu(9)#1	61.95(4)	C(23)-Cu(4)-Cu(1)#2	145.9(2)	C(68)-Cu(7)-Cu(8)	105.87(19)
C(68)-Cu(7)-Cu(9)	48.45(19)	C(76)-Cu(8)-C(83)#1	141.2(3)	C(83)#1-Cu(8)-Cu(9)#1	80.69(19)
C(68)-Cu(7)-N(8)	119.7(3)	C(76)-Cu(8)-C(84)#1	105.8(3)	C(84)#1-Cu(6)-C(75)#1	129.1(3)
C(68)-Cu(7)-N(9)	122.2(2)	C(76)-Cu(8)-Cu(6)	103.06(19)	C(84)#1-Cu(6)-C(83)#1	33.4(2)
C(68)-Cu(9)-C(84)	100.6(3)	C(76)-Cu(8)-Cu(7)	98.57(18)	C(84)#1-Cu(6)-Cu(7)	107.62(18)
C(68)-Cu(9)-Cu(10)	51.76(18)	C(76)-Cu(8)-Cu(9)	47.10(18)	C(84)#1-Cu(6)-Cu(8)	48.43(18)
C(68)-Cu(9)-Cu(6)	91.79(18)	C(76)-Cu(8)-Cu(9)#1	60.79(19)	C(84)#1-Cu(6)-Cu(9)	91.75(17)
C(68)-Cu(9)-Cu(6)#1	147.21(18)	C(76)-Cu(9)-C(68)	144.5(3)	C(84)#1-Cu(6)-Cu(9)#1	52.00(18)
C(68)-Cu(9)-Cu(7)	46.51(18)	C(76)-Cu(9)-C(84)	101.1(2)	C(84)#1-Cu(8)-Cu(6)	51.31(18)
C(68)-Cu(9)-Cu(8)	111.85(19)	C(76)-Cu(9)-Cu(10)	135.62(18)	C(84)#1-Cu(8)-Cu(7)	115.01(19)
C(68)-Cu(9)-Cu(8)#1	117.2(2)	C(76)-Cu(9)-Cu(6)	96.80(18)	C(84)#1-Cu(8)-Cu(9)	102.17(19)
C(68)-Cu(9)-Cu(9)#1	143.81(19)	C(76)-Cu(9)-Cu(6)#1	50.72(18)	C(84)#1-Cu(8)-Cu(9)#1	47.12(19)
C(75)#1-Cu(6)-C(83)#1	162.0(2)	C(76)-Cu(9)-Cu(7)	107.82(19)	C(84)-Cu(10)-C(67)	144.4(3)
C(75)#1-Cu(6)-Cu(7)	104.20(18)	C(76)-Cu(9)-Cu(8)	48.93(18)	C(84)-Cu(10)-C(68)	108.4(3)
C(75)#1-Cu(6)-Cu(8)	130.89(19)	C(76)-Cu(9)-Cu(8)#1	97.82(19)	C(84)-Cu(10)-Cu(9)	57.45(19)
C(75)#1-Cu(6)-Cu(9)	76.97(18)	C(76)-Cu(9)-Cu(9)#1	62.35(19)	C(84)-Cu(9)-Cu(10)	49.62(17)
C(75)#1-Cu(6)-Cu(9)#1	79.89(18)	C(83)#1-Cu(6)-Cu(7)	89.66(17)	C(84)-Cu(9)-Cu(6)	127.56(18)
C(76)#1-Cu(6)-C(75)#1	33.6(3)	C(83)#1-Cu(6)-Cu(8)	47.38(17)	C(84)-Cu(9)-Cu(6)#1	51.14(18)
C(76)#1-Cu(6)-C(83)#1	130.9(2)	C(83)#1-Cu(6)-Cu(9)	103.41(17)	C(84)-Cu(9)-Cu(7)	147.12(18)
C(76)#1-Cu(6)-C(84)#1	97.9(3)	C(83)#1-Cu(6)-Cu(9)#1	84.42(17)	C(84)-Cu(9)-Cu(8)	147.27(18)
C(76)#1-Cu(6)-Cu(7)	108.37(18)	C(83)#1-Cu(8)-C(84)#1	35.8(3)	C(84)-Cu(9)-Cu(8)#1	43.96(17)
C(76)#1-Cu(6)-Cu(8)	102.73(18)	C(83)#1-Cu(8)-Cu(6)	53.44(18)	C(84)-Cu(9)-Cu(9)#1	92.22(18)
C(76)#1-Cu(6)-Cu(9)	60.68(18)	C(83)#1-Cu(8)-Cu(7)	97.08(18)	C(83)#1-Cu(8)-Cu(9)	119.71(19)
C(76)#1-Cu(6)-Cu(9)#1	46.61(18)				

Symmetry transformations used to generate equivalent atoms:

#1 -x+1,-y+1,-z+1 #2 -x+1,-y+1,-z

Table S7. Selected bond length (Å) and bond angles (°) of $\mathbf{Cu_{18}}$.

Cu(8)-Cu(6)	2.9923(14)	Cu(6)-N(1)	2.017(6)	Cu(4)-C(9)	1.986(7)
Cu(5)-Cu(1)	2.9252(13)	Cu(3)-N(3)	1.972(6)	Cu(5)-C(41)	2.111(7)
Cu(7)-Cu(8)#1	2.8718(15)	Cu(5)-N(5)	1.972(5)	Cu(5)-C(42)	2.055(6)
Cu(2)-Cu(1)	2.8412(15)	Cu(9)-N(6)	1.971(6)	Cu(5)-C(54)	2.434(7)
Cu(9)-Cu(8)	2.7335(13)	Cu(2)-N(4)	1.958(6)	Cu(5)-C(55)	2.191(6)
Cu(7)-Cu(3)#1	2.7302(14)	Cu(1)-N(2)	1.891(6)	Cu(6)-C(8)	2.031(7)
Cu(4)-Cu(8)	2.7174(13)	Cu(1)-C(42)	1.852(7)	Cu(6)-C(9)	2.141(7)
Cu(4)-Cu(7)#1	2.7096(14)	Cu(2)-C(10)	2.509(7)	Cu(7)-C(29)#1	2.428(9)
Cu(4)-Cu(9)	2.7056(12)	Cu(2)-C(41)	2.255(7)	Cu(7)-C(56)	1.919(7)
Cu(4)-Cu(2)	2.7018(13)	Cu(2)-C(42)	2.023(7)	Cu(7)-C(8)	1.934(7)

Cu(7)-Cu(9)#1	2.6884(13)	Cu(2)-C(9)	2.316(6)	Cu(8)-C(55)	2.042(7)
Cu(4)-Cu(5)	2.6625(13)	Cu(3)-C(29)	2.182(12)	Cu(8)-C(56)	2.035(7)
Cu(4)-Cu(3)	2.6406(14)	Cu(3)-C(56)#1	2.047(6)	Cu(8)-C(7)#1	2.380(7)
Cu(7)-Cu(6)	2.5600(13)	Cu(3)-C(57)#1	2.119(7)	Cu(8)-C(8)#1	2.175(7)
Cu(4)-Cu(6)	2.5263(13)	Cu(4)-C(29)	2.000(12)	Cu(9)-C(29)	2.129(15)
Cu(7)-Cu(8)	2.4905(13)	Cu(4)-C(55)	1.993(7)	Cu(9)-C(7)#1	2.074(7)
Cu(9)-C(8)#1	2.128(6)	N(1)-Cu(6)-C(8)	117.4(2)	C(10)-Cu(2)-Cu(1)	69.76(17)
Cu(2)-Cu(1)-Cu(5)	66.21(4)	N(1)-Cu(6)-C(9)	107.7(3)	C(10)-Cu(2)-Cu(4)	74.76(15)
Cu(2)-Cu(4)-Cu(7)#1	133.06(5)	N(1)-Cu(6)-Cu(4)	125.90(16)	C(29)#1-Cu(7)-Cu(3)#1	49.6(3)
Cu(2)-Cu(4)-Cu(8)	162.95(5)	N(1)-Cu(6)-Cu(7)	109.16(17)	C(29)#1-Cu(7)-Cu(4)#1	45.4(3)
Cu(2)-Cu(4)-Cu(9)	122.92(4)	N(1)-Cu(6)-Cu(8)	120.82(18)	C(29)#1-Cu(7)-Cu(6)	149.5(3)
Cu(3)#1-Cu(7)-Cu(8)#1	115.18(4)	N(2)-Cu(1)-Cu(2)	139.8(2)	C(29)#1-Cu(7)-Cu(8)	135.9(2)
Cu(3)-Cu(4)-Cu(2)	72.94(4)	N(2)-Cu(1)-Cu(5)	133.9(2)	C(29)#1-Cu(7)-Cu(8)#1	90.9(4)
Cu(3)-Cu(4)-Cu(5)	132.22(4)	N(3)-Cu(3)-C(29)	100.8(4)	C(29)#1-Cu(7)-Cu(9)#1	48.8(3)
Cu(3)-Cu(4)-Cu(7)#1	61.35(4)	N(3)-Cu(3)-C(56)#1	151.6(3)	C(29)-Cu(3)-Cu(4)	47.9(3)
Cu(3)-Cu(4)-Cu(8)	123.96(5)	N(3)-Cu(3)-C(57)#1	117.6(3)	C(29)-Cu(3)-Cu(7)#1	58.0(3)
Cu(3)-Cu(4)-Cu(9)	99.57(5)	N(3)-Cu(3)-Cu(4)	114.83(19)	C(29)-Cu(4)-Cu(2)	85.6(3)
Cu(4)#1-Cu(7)-Cu(3)#1	58.08(3)	N(3)-Cu(3)-Cu(7)#1	156.30(17)	C(29)-Cu(4)-Cu(3)	54.0(4)
Cu(4)#1-Cu(7)-Cu(8)#1	58.18(3)	N(4)-Cu(2)-C(10)	94.6(2)	C(29)-Cu(4)-Cu(5)	91.9(3)
Cu(4)-Cu(2)-Cu(1)	71.16(4)	N(4)-Cu(2)-C(41)	121.2(2)	C(29)-Cu(4)-Cu(6)	153.7(3)
Cu(4)-Cu(3)-Cu(7)#1	60.57(4)	N(4)-Cu(2)-C(42)	152.0(3)	C(29)-Cu(4)-Cu(7)#1	59.8(2)
Cu(4)-Cu(5)-Cu(1)	70.38(4)	N(4)-Cu(2)-C(9)	105.3(2)	C(29)-Cu(4)-Cu(8)	105.9(4)
Cu(4)-Cu(6)-Cu(7)	106.37(4)	N(4)-Cu(2)-Cu(1)	162.07(18)	C(29)-Cu(4)-Cu(9)	51.1(4)
Cu(4)-Cu(6)-Cu(8)	58.27(3)	N(4)-Cu(2)-Cu(4)	114.20(18)	C(29)-Cu(9)-C(8)#1	104.6(3)
Cu(4)-Cu(8)-Cu(6)	52.25(3)	N(5)-Cu(5)-C(41)	113.7(2)	C(29)-Cu(9)-Cu(4)	47.0(3)
Cu(4)-Cu(8)-Cu(7)#1	57.92(3)	N(5)-Cu(5)-C(42)	147.4(3)	C(29)-Cu(9)-Cu(7)#1	59.2(2)
Cu(4)-Cu(8)-Cu(9)	59.52(3)	N(5)-Cu(5)-C(54)	98.9(2)	C(29)-Cu(9)-Cu(8)	101.7(3)
Cu(4)-Cu(9)-Cu(8)	59.95(3)	N(5)-Cu(5)-C(55)	105.9(2)	C(41)-Cu(2)-C(10)	143.4(2)
Cu(5)-Cu(4)-Cu(2)	71.92(4)	N(5)-Cu(5)-Cu(1)	168.88(18)	C(41)-Cu(2)-C(9)	129.9(2)
Cu(5)-Cu(4)-Cu(7)#1	133.83(4)	N(5)-Cu(5)-Cu(4)	114.78(17)	C(41)-Cu(2)-Cu(1)	73.67(18)
Cu(5)-Cu(4)-Cu(8)	94.75(4)	N(6)-Cu(9)-C(29)	110.9(3)	C(41)-Cu(2)-Cu(4)	94.98(17)
Cu(5)-Cu(4)-Cu(9)	74.30(4)	N(6)-Cu(9)-C(7)#1	109.7(3)	C(41)-Cu(5)-C(54)	144.7(3)
Cu(6)-Cu(4)-Cu(2)	105.65(4)	N(6)-Cu(9)-C(8)#1	144.4(3)	C(41)-Cu(5)-C(55)	137.3(3)
Cu(6)-Cu(4)-Cu(3)	105.89(5)	N(6)-Cu(9)-Cu(4)	113.10(16)	C(41)-Cu(5)-Cu(1)	73.73(19)
Cu(6)-Cu(4)-Cu(5)	114.03(5)	N(6)-Cu(9)-Cu(7)#1	170.06(18)	C(41)-Cu(5)-Cu(4)	99.70(19)
Cu(6)-Cu(4)-Cu(7)#1	96.83(4)	N(6)-Cu(9)-Cu(8)	120.52(19)	C(42)-Cu(1)-Cu(2)	45.2(2)
Cu(6)-Cu(4)-Cu(8)	69.48(4)	C(42)-Cu(1)-Cu(5)	44.2(2)	C(55)-Cu(8)-Cu(4)	46.92(19)
Cu(6)-Cu(4)-Cu(9)	129.94(5)	C(42)-Cu(1)-N(2)	174.9(3)	C(55)-Cu(8)-Cu(6)	61.25(19)
Cu(6)-Cu(7)-Cu(3)#1	159.31(5)	C(42)-Cu(2)-C(10)	110.1(3)	C(55)-Cu(8)-Cu(7)	110.49(19)
Cu(6)-Cu(7)-Cu(4)#1	136.98(5)	C(42)-Cu(2)-C(41)	33.4(3)	C(55)-Cu(8)-Cu(7)#1	103.94(19)
Cu(6)-Cu(7)-Cu(8)#1	78.99(4)	C(42)-Cu(2)-C(9)	102.7(3)	C(55)-Cu(8)-Cu(9)	75.72(18)
Cu(6)-Cu(7)-Cu(9)#1	102.63(4)	C(42)-Cu(2)-Cu(1)	40.6(2)	C(56)#1-Cu(3)-C(29)	102.3(3)
Cu(7)#1-Cu(4)-Cu(8)	63.90(4)	C(42)-Cu(2)-Cu(4)	85.86(18)	C(56)#1-Cu(3)-C(57)#1	34.9(3)
Cu(7)#1-Cu(8)-Cu(6)	83.82(4)	C(42)-Cu(5)-C(41)	34.8(3)	C(56)#1-Cu(3)-Cu(4)	93.0(2)

Cu(7)#1-Cu(9)-Cu(4)	60.31(3)	C(42)-Cu(5)-C(54)	110.3(3)	C(56)#1-Cu(3)-Cu(7)#1	44.6(2)
Cu(7)#1-Cu(9)-Cu(8)	63.96(4)	C(42)-Cu(5)-C(55)	106.6(3)	C(56)-Cu(7)-C(29)#1	97.8(4)
Cu(7)-Cu(6)-Cu(8)	52.60(3)	C(42)-Cu(5)-Cu(1)	39.0(2)	C(56)-Cu(7)-C(8)	161.5(3)
Cu(7)-Cu(8)-Cu(4)	102.78(4)	C(42)-Cu(5)-Cu(4)	86.29(19)	C(56)-Cu(7)-Cu(3)#1	48.47(19)
Cu(7)-Cu(8)-Cu(6)	54.75(3)	C(54)-Cu(5)-Cu(1)	72.15(16)	C(56)-Cu(7)-Cu(4)#1	93.9(2)
Cu(7)-Cu(8)-Cu(7)#1	93.84(4)	C(54)-Cu(5)-Cu(4)	77.27(18)	C(56)-Cu(7)-Cu(6)	111.1(2)
Cu(7)-Cu(8)-Cu(9)	150.68(5)	C(55)-Cu(4)-C(29)	125.4(4)	C(56)-Cu(7)-Cu(8)	53.1(2)
Cu(8)-Cu(7)-Cu(3)#1	92.56(4)	C(55)-Cu(4)-Cu(2)	114.65(19)	C(56)-Cu(7)-Cu(8)#1	128.0(2)
Cu(8)-Cu(7)-Cu(4)#1	98.68(4)	C(55)-Cu(4)-Cu(3)	172.38(19)	C(56)-Cu(7)-Cu(9)#1	146.2(2)
Cu(8)-Cu(7)-Cu(6)	72.65(4)	C(55)-Cu(4)-Cu(5)	53.86(18)	C(56)-Cu(8)-C(55)	116.8(3)
Cu(8)-Cu(7)-Cu(8)#1	86.16(4)	C(55)-Cu(4)-Cu(6)	72.01(19)	C(56)-Cu(8)-C(7)#1	109.3(3)
Cu(8)-Cu(7)-Cu(9)#1	144.58(5)	C(55)-Cu(4)-Cu(7)#1	111.31(19)	C(56)-Cu(8)-C(8)#1	117.1(3)
Cu(9)#1-Cu(7)-Cu(3)#1	97.78(4)	C(55)-Cu(4)-Cu(8)	48.43(19)	C(56)-Cu(8)-Cu(4)	145.2(2)
Cu(9)#1-Cu(7)-Cu(4)#1	60.16(3)	C(55)-Cu(4)-Cu(9)	77.10(19)	C(56)-Cu(8)-Cu(6)	93.2(2)
Cu(9)#1-Cu(7)-Cu(8)#1	58.78(3)	C(55)-Cu(5)-C(54)	30.3(3)	C(56)-Cu(8)-Cu(7)	48.9(2)
Cu(9)-Cu(4)-Cu(7)#1	59.53(3)	C(55)-Cu(5)-Cu(1)	69.81(17)	C(56)-Cu(8)-Cu(7)#1	131.5(2)
Cu(9)-Cu(4)-Cu(8)	60.54(3)	C(55)-Cu(5)-Cu(4)	47.28(18)	C(56)-Cu(8)-Cu(9)	154.9(2)
Cu(9)-Cu(8)-Cu(6)	111.72(4)	C(55)-Cu(8)-C(7)#1	115.7(2)	C(57)#1-Cu(3)-C(29)	134.8(3)
Cu(9)-Cu(8)-Cu(7)#1	57.26(4)	C(55)-Cu(8)-C(8)#1	124.7(3)	C(57)#1-Cu(3)-Cu(4)	122.75(19)
C(57)#1-Cu(3)-Cu(7)#1	78.95(18)	C(8)#1-Cu(8)-Cu(7)#1	42.31(19)	C(8)-Cu(7)-Cu(9)#1	51.75(19)
C(7)#1-Cu(8)-Cu(4)	105.35(18)	C(8)#1-Cu(8)-Cu(9)	49.81(16)	C(9)-Cu(2)-C(10)	28.9(2)
C(7)#1-Cu(8)-Cu(6)	154.09(19)	C(8)#1-Cu(9)-Cu(4)	92.48(18)	C(9)-Cu(2)-Cu(1)	65.33(18)
C(7)#1-Cu(8)-Cu(7)	133.68(16)	C(8)#1-Cu(9)-Cu(7)#1	45.52(19)	C(9)-Cu(2)-Cu(4)	45.83(17)
C(7)#1-Cu(8)-Cu(7)#1	71.79(19)	C(8)#1-Cu(9)-Cu(8)	51.32(19)	C(9)-Cu(4)-C(29)	119.0(5)
C(7)#1-Cu(8)-Cu(9)	47.23(17)	C(8)-Cu(6)-C(9)	111.9(3)	C(9)-Cu(4)-C(55)	114.1(3)
C(7)#1-Cu(9)-C(29)	139.4(3)	C(8)-Cu(6)-Cu(4)	116.7(2)	C(9)-Cu(4)-Cu(2)	56.78(18)
C(7)#1-Cu(9)-C(8)#1	34.8(3)	C(8)-Cu(6)-Cu(7)	48.1(2)	C(9)-Cu(4)-Cu(3)	68.9(2)
C(7)#1-Cu(9)-Cu(4)	115.62(19)	C(8)-Cu(6)-Cu(8)	90.87(19)	C(9)-Cu(4)-Cu(5)	114.5(2)
C(7)#1-Cu(9)-Cu(7)#1	80.3(2)	C(8)-Cu(7)-C(29)#1	100.5(4)	C(9)-Cu(4)-Cu(6)	55.11(19)
C(7)#1-Cu(9)-Cu(8)	57.4(2)	C(8)-Cu(7)-Cu(3)#1	149.22(19)	C(9)-Cu(4)-Cu(7)#1	111.2(2)
C(8)#1-Cu(8)-C(7)#1	31.6(3)	C(8)-Cu(7)-Cu(4)#1	96.9(2)	C(9)-Cu(4)-Cu(8)	123.77(18)
C(8)#1-Cu(8)-Cu(4)	91.14(18)	C(8)-Cu(7)-Cu(6)	51.47(19)	C(9)-Cu(4)-Cu(9)	168.3(2)
C(8)#1-Cu(8)-Cu(6)	125.94(19)	C(8)-Cu(7)-Cu(8)	110.17(19)	C(9)-Cu(6)-Cu(4)	49.52(18)
C(8)#1-Cu(8)-Cu(7)	113.27(17)	C(8)-Cu(7)-Cu(8)#1	49.2(2)	C(9)-Cu(6)-Cu(7)	143.1(2)
C(9)-Cu(6)-Cu(8)	107.19(18)				

Symmetry transformations used to generate equivalent atoms:

#1 -x+1,-y+1,-z+1 #2 -x+1,-y+1,-z

Reference

1. G. M. Sheldrick, *SHELXT*– Integrated space-group and crystal-structure determination, *Acta Crystallogr., Sect. A: Found. Adv.*, 2015, **71**, 3-8.
2. O. V. Dolomanov, L. J. Bourhis, R. J. Gildea, J. A. K. Howard and H. Puschmann, OLEX2: a complete structure solution, refinement and analysis program, *J. Appl. Crystallogr.*, 2009, **42**, 339-341.

3. G. M. Sheldrick, Crystal structure refinement with *SHELXL*, *Acta Crystallogr., Sect. C: Struct. Chem.*, 2015, **71**, 3-8.
4. S. A. P. a. Z. W. H. V. R. Dias, Coinage metal complexes of 3,5-bis(trifluoromethyl)pyrazolate ligand synthesis and characterization of $\{[3,5\text{-}(CF_3)_2Pz]Cu\}_3$ and $\{[3,5\text{-}(CF_3)_2Pz]Ag\}_3$, *J. Fluor. Chem.*, 2000, **103**, 163–169.
5. A. Eichhöfer, G. Buth, S. Lebedkin, M. Kühn and F. Weigend, Luminescence in phosphine-stabilized copper chalcogenide cluster molecules—a comparative study, *Inorg. Chem.*, 2015, **54**, 9413-9422.
6. Q. Benito, X. F. Le Goff, S. Maron, A. Fargues, A. Garcia, C. Martineau, F. Taulelle, S. Kahlal, T. Gacoin, J.-P. Boilot and S. Perruchas, Polymorphic copper Iodide clusters: Insights into the mechanochromic luminescence properties, *J. Am. Chem. Soc.*, 2014, **136**, 11311-11320.
7. Q. Benito, X. F. Le Goff, G. Nocton, A. Fargues, A. Garcia, A. Berhault, S. Kahlal, J.-Y. Saillard, C. Martineau, J. Trébosc, T. Gacoin, J.-P. Boilot and S. Perruchas, Geometry flexibility of copper Iodide clusters: variability in luminescence thermochromism, *Inorg. Chem.*, 2015, **54**, 4483-4494.
8. H. Li, H. Zhai, C. Zhou, Y. Song, F. Ke, W. W. Xu and M. Zhu, Atomically precise copper cluster with Intensely near-Infrared luminescence and Its mechanism, *J. Phys. Chem. Lett.* , 2020, **11**, 4891-4896.
9. X.-X. Yang, I. Issac, S. Lebedkin, M. Kühn, F. Weigend, D. Fenske, O. Fuhr and A. Eichhöfer, Red-luminescent biphosphine stabilized '$Cu_{12}S_6$' cluster molecules, *Chem. Commun.*, 2014, **50**, 11043-11045.
10. K. Zhang, Y. Shen, X. Yang, J. Liu, T. Jiang, N. Finney, B. Spingler and S. Duttwyler, Atomically defined monocarborane copper(I) acetylides with structural and luminescence properties tuned by ligand sterics, *Chem. Eur.J.* , 2019, **25**, 8754 –8759.
11. Y. L. Li, J. Wang, P. Luo, X. H. Ma, X. Y. Dong, Z. Y. Wang, C. X. Du, S. Q. Zang and T. C. W. Mak, Cu_{14} cluster with partial Cu(0) character: difference in electronic structure from Isostructural silver analog, *Adv. Sci.* , 2019, **6**, 1900833.
12. M. Olaru, E. Rychagova, S. Ketkov, Y. Shynkarenko, S. Yakunin, M. V. Kovalenko, A. Yablonskiy, B. Andreev, F. Kleemiss, J. Beckmann and M. Vogt, A small cationic organo-copper cluster as thermally robust highly photo- and electroluminescent material, *J. Am. Chem. Soc.*, 2020, **142**, 373-381.
13. I. S. Krytchankou, I. O. Koshevoy, V. V. Gurzhiy, V. A. Pomogaev and S. P. Tunik, Luminescence solvato- and vapochromism of alkynyl-phosphine copper clusters, *Inorg. Chem.*, 2015, **54**, 8288-8297.
14. X.-Y. Chang, K.-H. Low, J.-Y. Wang, J.-S. Huang and C.-M. Che, From cluster to polymer: Ligand cone angle controlled syntheses and structures of copper(I) alkynyl complexes, *Angew. Chem., Int. Ed.*, 2016, **55**, 10312-10316.
15. M.-M. Zhang, X.-Y. Dong, Z.-Y. Wang, H.-Y. Li, S.-J. Li, X. Zhao and S.-Q. Zang, AIE triggers the circularly polarized luminescence of atomically precise enantiomeric copper(I) alkynyl clusters, *Angew. Chem., Int. Ed.*, 2020, **59**, 10052-10058.
16. S.-L. Li, F.-Q. Zhang and X.-M. Zhang, An organic-ligand-free thermochromic luminescent cuprous iodide trinuclear cluster: evidence for cluster centered emission and configuration distortion with temperature, *Chem. Commun.*, 2015, **51**, 8062-8065.
17. G. te Velde, F. M. Bickelhaupt, E. J. Baerends, C. Fonseca Guerra, S. J. A. van Gisbergen, J. G. Snijders and T. Ziegler, Chemistry with ADF, *J. Comput. Chem.*, 2001, **22**, 931-967.
18. C. Fonseca Guerra, J. G. Snijders, G. te Velde and E. J. Baerends, Towards an order-N DFT method, *Theor. Chem. Account.*, 1998, **99**, 391-403.
19. S. Grimme, J. Antony, S. Ehrlich and H. Krieg, A consistent and accurate *ab initio* parametrization of density functional dispersion correction (DFT-D) for the 94 elements H-Pu, *J. Chem. Phys.* , 2010, **132**, 154104.
20. E. Van Lenthe and E. J. Baerends, Optimized Slater-type basis sets for the elements 1–118, *J. Comput. Chem.*, 2003, **24**, 1142-1156.

21. M. J. Frisch, G. W. Trucks, H. B. Schlegel, G. E. Scuseria, M. A. Robb, J. R. Cheeseman, G. Scalmani, V. Barone, G. A. Petersson, H. Nakatsuji, X. Li, M. Caricato, A. V. Marenich, J. Bloino, B. G. Janesko, R. Gomperts, B. Mennucci, H. P. Hratchian, J. V. Ortiz, A. F. Izmaylov, J. L. Sonnenberg, Williams, F. Ding, F. Lipparini, F. Egidi, J. Goings, B. Peng, A. Petrone, T. Henderson, D. Ranasinghe, V. G. Zakrzewski, J. Gao, N. Rega, G. Zheng, W. Liang, M. Hada, M. Ehara, K. Toyota, R. Fukuda, J. Hasegawa, M. Ishida, T. Nakajima, Y. Honda, O. Kitao, H. Nakai, T. Vreven, K. Throssell, J. A. Montgomery Jr., J. E. Peralta, F. Ogliaro, M. J. Bearpark, J. J. Heyd, E. N. Brothers, K. N. Kudin, V. N. Staroverov, T. A. Keith, R. Kobayashi, J. Normand, K. Raghavachari, A. P. Rendell, J. C. Burant, S. S. Iyengar, J. Tomasi, M. Cossi, J. M. Millam, M. Klene, C. Adamo, R. Cammi, J. W. Ochterski, R. L. Martin, K. Morokuma, O. Farkas, J. B. Foresman and D. J. Fox, Gaussian 16 Rev. C.01.*Journal*, 2016.
22. F. Weigend and R. Ahlrichs, Balanced basis sets of split valence, triple zeta valence and quadruple zeta valence quality for H to Rn: Design and assessment of accuracy, *Phys. Chem. Chem. Phys.*, 2005, **7**, 3297-3305.
23. T. Lu and F. Chen, Multiwfn: A multifunctional wavefunction analyzer, *J. Comput. Chem.*, 2012, **33**, 580-592.
24. W. Humphrey, A. Dalke and K. Schulten, VMD: Visual molecular dynamics, *J. Mol. Graphics*, 1996, **14**, 33-38.
25. J. F. Rudzinski, K. Kremer and T. Bereau, Communication: Consistent interpretation of molecular simulation kinetics using Markov state models biased with external information, *J. Chem. Phys.*, 2016, **144**, 051102.
26. E. v. Lenthe, E. J. Baerends and J. G. Snijders, Relativistic total energy using regular approximations, *J. Chem. Phys.*, 1994, **101**, 9783-9792.
27. E. v. Lenthe, E. J. Baerends and J. G. Snijders, Relativistic regular two-component Hamiltonians, *J. Chem. Phys.*, 1993, **99**, 4597-4610.
28. E. v. Lenthe, J. G. Snijders and E. J. Baerends, The zero-order regular approximation for relativistic effects: The effect of spin–orbit coupling in closed shell molecules, *J. Chem. Phys.*, 1996, **105**, 6505-6516.